SECTION B7.3

BENDING ANALYSIS OF

TABLE OF CONTENTS

B7.3.0 BENDING ANALYSIS OF THIN SHELLS

In this section some of the theories discussed in Section B7.0 will be applied to solve shell problems. Section B7.0 defined the structural shell and several shell theories, with their limitations and ramifications. It was pointed out that the thickness-to-radius-of-curvature ratio, material behavior, type of construction (e.g., honeycomb sandwich or ring-stiffened shells), types of loading, and other factors all play a role in establishing which theory is applicable. Furthermore, shallow versus nonshallow shells required different approaches even though they fell into the same thin shell theory.

In this section, differential equations and their solutions will be tabulated for simple and complex rotationally symmetric geometries subjected to arbitrary rotationally symmetric loads. There are certain restraining conditions, called edge restraints, that the solution must satisfy. The edge restraints are reduced to unit loads and, by making the solution of the differential equations satisfy these unit edge restraints, the influence coefficients for the geometry are obtained. These influence coefficients, etc., are then used to solve problems that involve determining stresses, strains, and displacements in simple and complex geometries.

The procedure for bending analysis of thin shells will be as follows: The surface loads, inertia loads, and thermally induced loads are included in the equilibrium equations and will be part of the "membrane solution" using Section B7.1. The solution due to edge restraints alone is then found and the results superimposed over the membrane solution. The results obtained will be essentially identical to those obtained by using the complete, exact bending theory.

B7.3.1 GENERAL

The geometry, coordinates, stresses, and stress resultants for a shell of revolution are the same as given in Paragraph B7.1.1.0. Also, the notations and sign conventions are generally the same as those given in Paragraph B7.1.1.1 and Paragraph B7.1.1.2, respectively. The limitations of analysis are the same as given in Paragraph B7.1.1.3, except that in this section flexural strains, stresses, and stress resultants are no longer zero. Boundaries of the shell need not be free to rotate and deflect normal to the shell middle surface.

B7.3.1.1 Equations

I Equilibrium Equations

A shell element with the stress resultants as given in Section B7.1.1.0 will now be considered and the conditions for its equilibrium under the influence of all external and internal loads will be determined. The equations arising by virtue of the demands of equilibrium and the compatibility of deformations will be derived by considering an individual differential element.

The external loads are comprised of body forces that act on the element and surface forces (stresses) that act on the upper and lower boundaries of the element, which are sections of the curved surfaces bounding the shell. The internal forces will be stress resultants acting on the faces of the shell element.

For the following equations, external forces are replaced by statically equivalent stresses distributed at the middle surfaces. The middle surface is thus loaded by forces as well as moments.

Now, instead of considering the equilibrium of an element of a shell one may study the equilibrium of the corresponding element of the middle surface. The stresses, in general, vary from point to point in the shell, and as a result the stress resultants will also vary.

Consider the stress resultants of concern applied to the middle surface of the shell as shown in Figures B7.3.1-1 and B7.3.1-2.

The equilibrium of the shell, in the θ, ϕ, and z coordinate directions respectively, is given by the following equations:

$$\frac{\partial \alpha_2 N_\theta}{\partial \theta} + \frac{\partial \alpha_1 N_{\phi\theta}}{\partial \phi} + N_{\theta\phi}\frac{\partial \alpha_1}{\partial \phi} - N_\phi \frac{\partial \alpha_2}{\partial \theta} + Q_\theta \frac{\alpha_1 \alpha_2}{R_1} + \alpha_1 \alpha_2 p_1 = 0$$

$$\frac{\partial \alpha_1 N_\phi}{\partial \phi} + \frac{\partial \alpha_2 N_{\theta\phi}}{\partial \theta} + N_{\phi\theta}\frac{\partial \alpha_2}{\partial \theta} - N_\theta \frac{\partial \alpha_1}{\partial \phi} + Q_\phi \frac{\alpha_1 \alpha_2}{R_2} + \alpha_1 \alpha_2 p_2 = 0$$

$$\frac{\partial \alpha_2 Q_\theta}{\partial \theta} + \frac{\partial \alpha_1 Q_\phi}{\partial \phi} - \alpha_1 \alpha_2 \left(\frac{N_\theta}{R_1} + \frac{N_\phi}{R_2}\right) + \alpha_1 \alpha_2 q = 0 \quad , \qquad (1a)$$

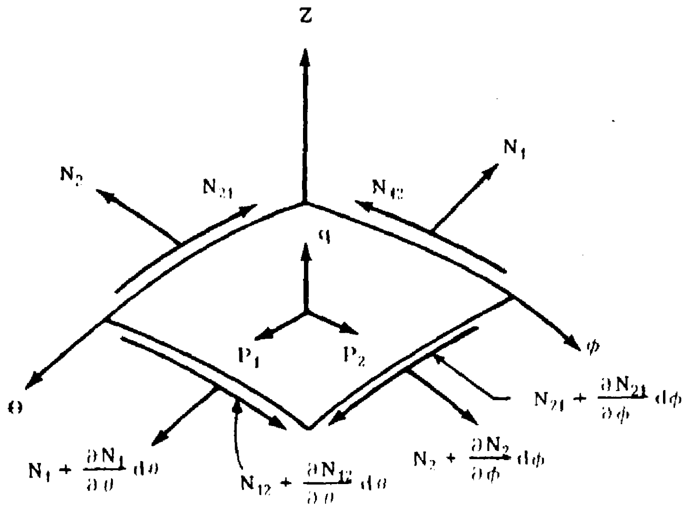

FIGURE B7.3.1-1 TYPICAL SHELL REFERENCE ELEMENT WITH AXIAL AND IN-PLANE SHEAR FORCES

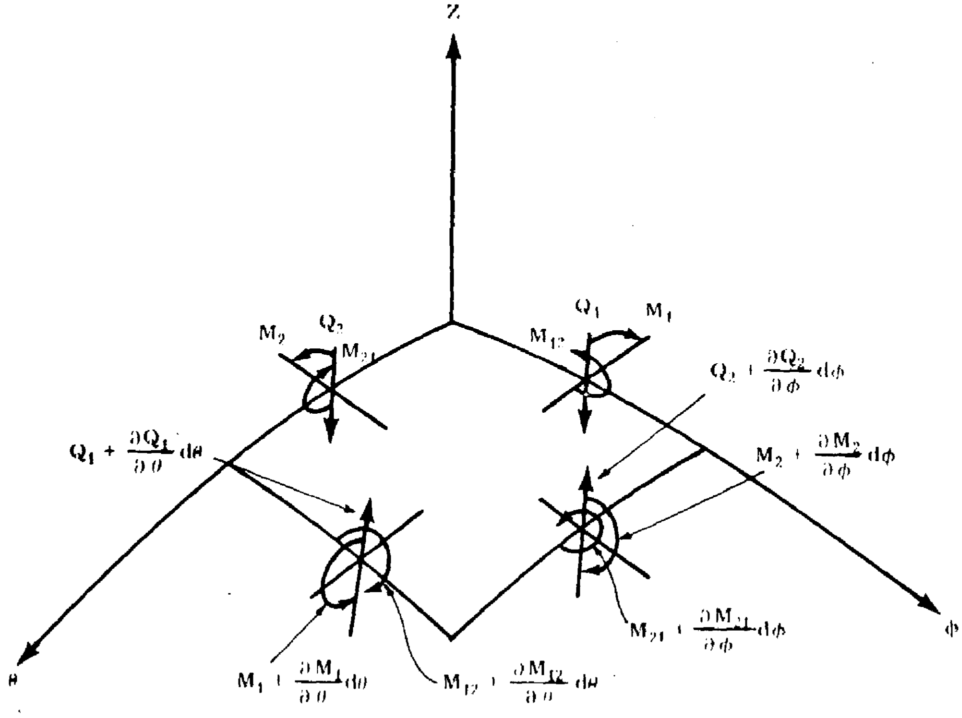

FIGURE B7.3.1-2 TYPICAL SHELL REFERENCE ELEMENT WITH TRANSVERSE SHEAR, BENDING, AND TWISTING ELEMENTS where p_1, p_2, and q are components of the effective external force per unit area applied to the middle surface of the shell.

The equilibrium of moments about the θ, ϕ, and z coordinates results in the following moment equilibrium expressions:

$$\frac{\partial \alpha_2}{\partial \theta} M_{\theta\phi} + \frac{\partial \alpha_1 M_\phi}{\partial \phi} - M_\theta \frac{\partial \alpha_1}{\partial \phi} + M_{\phi\theta} \frac{\partial \alpha_2}{\partial \theta} - Q_\phi \alpha_1 \alpha_2 = 0$$

$$\frac{\partial \alpha_1}{\partial \phi} M_{\phi\theta} + \frac{\partial \alpha_2 M_\theta}{\partial \theta} - M_\phi \frac{\partial \alpha_2}{\partial_\theta} + M_{\theta\phi} \frac{\partial \alpha_1}{\partial \phi} - Q_\theta \alpha_1 \alpha_2 = 0 \qquad (1b)$$

$$N_{\theta\phi} - N_{\phi\theta} + \frac{M_{\theta\phi}}{R_1} - \frac{M_{\phi\theta}}{R_2} = 0 \quad .$$

The force components of the last equilibrium expression are due to warping of the faces, and result from in-plane shears and twisting moments.

Now, for shells of revolution the resultant forces ($N_{\phi\theta}$, Q_θ) and moments ($M_{\phi\theta}$) vanish and $\alpha_1 = R_1$; $\alpha_2 = R_2 \sin \phi$. Therefore, the equilibrium equations become:

$$\frac{d(N_\phi R)}{d\phi} - N_\theta R_1 \cos \phi + Q_\phi R_1 + Rp = 0$$

$$\frac{d(Q_\phi R)}{d\phi} - N_\phi R_1 - N_\theta R_1 \sin \phi + R_1 R_q = 0 \qquad (2)$$

$$\frac{d(M_\phi R)}{d\phi} - M_\theta R_1 \cos \phi - R_1 R Q_\phi = 0$$

where the second, fourth, and sixth equations of (1) have been identically satisfied.

In the equilibrium equations presented here, changes in the dimensions and in the shape of the element of the middle surface arising from its deformation have been neglected. This simplification arises from the assumption of small deformations.

II Strain Displacement

For the particular case of axisymmetric deformations, the displacement (V) is zero, and all derivatives of displacement components with respect to θ vanish. In this case the middle surface strain-displacement equations become:

$$\epsilon_1^o = \epsilon_\phi^o = \frac{1}{R_1}\frac{du}{d\phi} + \frac{w}{R_1}$$

$$\epsilon_2^o = \epsilon_\theta^o = \frac{u\cot\phi}{R_1} + \frac{u dR_2}{R_1 R_2 d\phi} + \frac{w}{R_2} \tag{3}$$

$$\gamma_{12}^o = \gamma_{\phi\theta}^o = 0$$

and the curvature and twist expressions become

$$\kappa_1 = \kappa_\phi = -\frac{1}{R_1}\frac{d}{d\phi}\left(\frac{1}{R_1}\frac{dw}{d\phi} - \frac{u}{R_1}\right)$$

$$\kappa_2 = \kappa_\theta = -\frac{1}{R_1^2}\left[\cot\phi + \frac{1}{R_2}\frac{dR_2}{d\phi}\right]\left[\frac{dw}{d\phi} - u\right] . \tag{4}$$

$$\kappa_{12} = \kappa_{\phi\theta} = 0$$

for general surface of revolution, the expressions $\frac{dR}{d\phi}$ and $\frac{dR_2}{d\phi}$ are as follows for $R = R_2 \sin\phi$:

$$\frac{dR}{d\phi} = R_1 \cos\phi$$

$$\frac{dR_2}{d\phi} = (R_1 - R_2) \cot\phi \qquad (5)$$

inserting equation (5) into equation (3) yields

$$\epsilon_2 = \frac{u \cot\phi}{R_2} + \frac{w}{R_2}$$

$$\kappa_2 = -\frac{\cot\phi}{R_1 R_2}\left[\frac{dw}{d\phi} - u\right] \qquad (6)$$

while remaining strain-displacement equations of (3) and (4) are unchanged.

III <u>Stress-Strain Equations</u>

For an isotropic shell, the following constitutive equations relate stress resultants and couples to components of strain:

$$N_1 = \frac{Et}{1-\mu^2}\left(\epsilon_1^o + \mu\epsilon_2^o\right) \qquad M_1 = D[\kappa_1 + \mu\kappa_2]$$

$$N_2 = \frac{Et}{1-\mu^2}\left(\epsilon_2^o + \mu\epsilon_1^o\right) \qquad M_2 = D[\kappa_2 + \mu\kappa_1] \qquad (7)$$

$$N_{12} = N_{21} = \frac{Et}{2(1+\mu)}\ \gamma_{12}^o \qquad M_{12} = M_{21} = \frac{(1-\mu)}{2}\ D\,\kappa_{12}$$

where

$$D = \frac{Et^3}{12(1-\mu^2)}$$

and where (middle surface) strains (ϵ_1^o, ϵ_2^o, γ_{12}^o) are given in equation (3) and change in curvature and twist terms (κ_1, κ_2, κ_{12}) are given in equation (4).

IV Solution of Equations

By eliminating Q_ϕ from the first and last equilibrium equations (2) and determining the force resultants from equation (7), two second-order ordinary differential equations in the two unknown displacement components u and w are obtained. Rather than obtain equations in this manner, however, a transformation of dependent variables can be performed leading to a more manageable pair of equations, which for shells of constant meridional curvature and constant thickness, combine into a single fourth-order equation solvable in terms of a hypergeometric series.

The transformation to the Reissner-Meissner equations is accomplished by introducing, two new variables, the angular rotation

$$\tilde{V} = \frac{1}{R_1}\left(u - \frac{dw}{d\phi}\right)$$

and the quantity

$$\tilde{U} = R_2 Q_\phi \quad .$$

This substitution of variables leads to two second-order differential equations in $\tilde{U}$ and $\tilde{V}$ replacing the corresponding two equations in u and w. The details of this transformation are illustrated in Reference 1.

For shells of constant thickness and constant meridional curvature or, in fact, for any shell of revolution satisfying the Meissner condition, the transformed pair of equations can be combined into a single fourth-order equation, the solution of which is determined from the solution of a second-order complex equation. For shells of the description above, the shell equations can be represented in the simplified form:

$$L\left(\tilde{U} + \frac{u}{R_1}\ \tilde{U}\right) = Et\,\tilde{V}$$

$$L\left(\tilde{V}\right) - \frac{u}{R_1}\ \tilde{V} = -\frac{\tilde{U}}{D}$$

where the operator

$$L(\quad) = \frac{R_2}{R_1^2}\ \frac{d^2(\ )}{d\phi^2} + \frac{1}{R_1}\left[\frac{d}{d\phi}\ \left(\frac{R_2}{R_1}\right) + \frac{R_2}{R_1}\ \cot\phi\right]\frac{d(\ )}{d\phi} - \frac{R_1\cot^2\phi}{R_2 R_1}\ .$$

From the system shown above of two simultaneous differential equations of second order, an equation of fourth order is obtained for each unknown. Following operations described in Reference 1 yield an equation of the form

$$LL(\tilde{U}) + r^4\tilde{U} = 0$$

$$\Gamma^4 = \frac{Et}{D} - \frac{u^2}{R_1^2}\quad .$$

The solution of the fourth-order equation can be considered the solution of two second-order complex equations of the form

$$L(\tilde{U}) \pm i\ \ \Gamma^2\ \tilde{U} = 0\quad .$$

Reissner-Meissner type equations are the most convenient and most widely employed forms of the first approximation theory for axisymmetrically loaded shells of revolution. They follow exactly from the relations of Love's first approximation when the meridional curvature and thickness are constant, as they are for cylindrical, conical, spherical, and toroidal shells of uniform thickness. Furthermore, they follow directly from Love's equations in the more general case, provided that special restraints on the variation of thickness and geometry are satisfied.

B7.3.1.2 Unit Loading Method

Generally a shell is a statically indeterminate structure. The internal forces of the shell are determined from six equations of equilibrium, which are derived from the three-force and three-moment equilibrium conditions.

There are ten unknowns that make the problem internally statically indeterminate because determination of the unknowns does not depend on the supports. The situation is similar to one that occurs in a truss which, as used in practice, is a highly statically indeterminate system. If reactions to the applied loading can be found with the help of known equations of statical equilibrium, the system is externally determinate; however, a truss is a statically indeterminate system internally because, instead of the assumed simplification (which introduces hinges at the joints), all joints are welded or riveted together. This introduces the moment into the members. However, this additional influence is usually negligible. To find the statically indeterminate values, deformations must be considered.

The main objective of the following sections is to bypass the elaborate calculations by replacing the classical methods of elasticity theory with the simplified but accurate procedure called the unit loading method. This is accomplished by enforcing the conditions of equilibrium, compatibility in displacement, and rotations at the junctions.

I Comparison of Membrane and Bending Theories for Nonshallow Shells

As discussed in Sections B7.0 and B7.1, the bending theory is more general than the membrane theory because it permits use of all possible boundary conditions. To compare the two theories, assume a nonshallow spherical shell with some axisymmetrical loading built in along the edges. When the results are compared, the following conclusions can be made:

1. The stresses and deformations are almost identical for all locations of the shell with the exception of a narrow strip on the shell surface which is adjacent to the boundary. This narrow strip is generally no wider than $\sqrt{Rt}$, where R is the radius and t is the thickness of the spherical shell.

2. Except for the strip along the boundary, all bending moments, twisting moments, and vertical shears are negligible; this causes the entire solution to be practically identical to the membrane solution.

3. Disturbances along the supporting edge are very significant; however, the local bending and shear decrease rapidly along the meridian, and may become negligible outside of the narrow strip, as described in item 1.

Since the bending and membrane theories give practically the same results, except for a strip adjacent to the boundary, the simple membrane theory can be used; then, at the edges, the influence of moment and shear can be applied to bring the displaced edge of the shell into the position prescribed by boundary conditions. The bending theory is used for this operation. Consequently, once the solutions are obtained, they can be used later without any special derivation. The results obtained from application of both theories can be superimposed, which will lead to the final results being almost identical to those obtained by using the exact bending theory.

II Unit-Loading Method Applied to the Combined Theory

The solution of a shell of revolution under axisymmetrical loading can be conducted in a simplified way, known as the unit-loading method.

1. Assume that the shell under consideration is a free membrane. Obtain a solution for the overall stresses and distortions of the edges by using Section B7.1. This is the primary solution.

2. Apply the following edge loadings:

a. Moment in inch-pounds per inch along the edge

b. Horizontal shear in pounds per inch along the edge

c. Vertical shear in pounds per inch along the edge

These loadings should be of such magnitude as to be able to return the distorted edge of the membrane into a position prescribed by the nature of supports (edge condition). The third edge loading in the majority of cases is not necessary. The amount of applied corrective loadings depends on the magnitude of edge deformations due to the primary solution. The exact magnitude will be determined by the interaction procedure to be explained in Section B7.3.2. However, to start the interaction process, formulas will be necessary for deformations due to the following:

a. Unit-edge moment: M = 1 pound per inch

b. Unit-edge horizontal shear: Q = 1 pound per inch

c. Unit-edge vertical shear: V = 1 pound per inch.

These solutions will be referred to as unit-edge influences, or as secondary solutions.

3. Having the primary and unit-edge solutions, one can enter these into the interaction process. This process will determine the correct amount of corrective loadings (M, Q, and V); all stresses and distortions due to these loadings can consequently be determined.

4. Superposition of stresses and distortions obtained by primary solution and corrective loadings lead to the final solution.

B7.3.2 INTERACTION ANALYSIS

Missiles, space vehicles, and pressure vessels are examples of structural configurations usually consisting of various combinations of shell elements. For analysis, such complex shell configurations generally can be broken down into simple elements. However, at the intersection of these elements a discontinuity (point of abrupt change in geometry or loading) usually exists; that is, unknown shears and moments are introduced. The common shapes that a complex shell may be broken down to include spherical, elliptical, conical, toroidal; these shapes also occur in compound bulkheads. Figure

B7.3.2-1, for example, illustrates a compound bulkhead which consists of the spherical transition between the conical and cylindrical sections. For analysis of such a shell, the analyst must choose between two methods, depending on the accuracy required: (1) he can consider such a system as an irregular one and use some approximation, or (2) he can calculate it as a compound shell, using the method of interaction.

In this section, the interaction method is presented which is applicable not only to monocoque shells but also to sandwich and orthotropic shells. The interacting elements are often constructed from different materials. The loading can also vary considerably. The most frequently used loadings are internal or external pressure, axial tension or compression load, thermally induced loads, and the thrust loads.

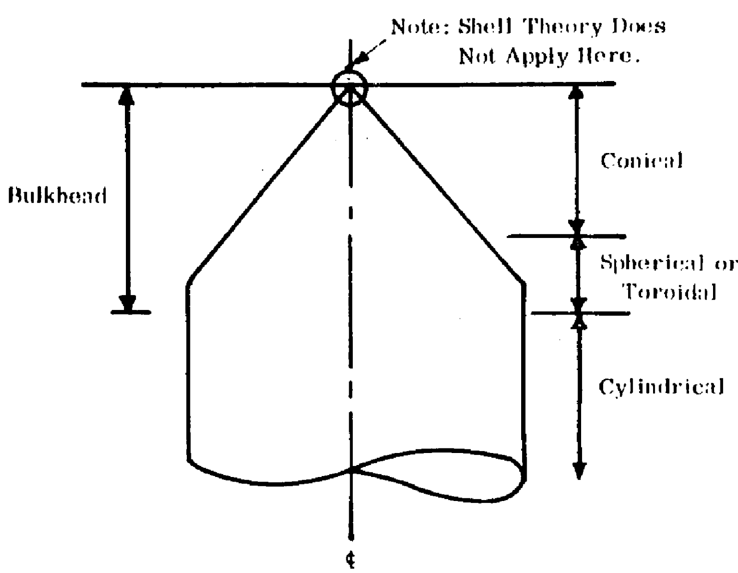

FIGURE B7.3.2-1 COMPOUND BULKHEAD

B7.3.2.1 Interaction Between Two Shell Elements

For simplicity, the interaction between two structural elements will be described first. The more general case of interaction of several elements, as is usually the case when the combined bulkhead is under consideration, will be described second. For the purpose of presentation, a system consisting of a bulkhead and cylinder, pressurized internally, is selected. The bulkhead can be considered as a unit element of some defined shape and will not be subdivided into separate portions in the great majority of cases. For example, assume the pressurized container to be theoretically separated into two main parts, the cylindrical shell and dome, as shown in Figure B7.3.2-2. Stresses and deformations introduced by internal pressure (or another external loading) can be determined for each part separately.

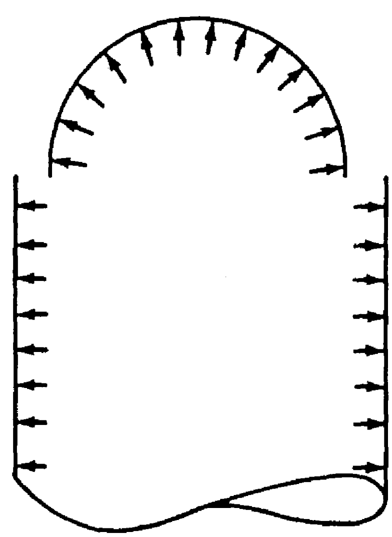

FIGURE B7.3.2-2 CYLINDRICAL SHELL AND DOME

Assume that the membrane analysis (primary solution) supplied the radial displacement ($\Delta r \doteq \delta_c$) and rotation (β_c) for the cylinder along the discontinuity line and $\Delta r = \delta_d$ and β_d for the dome. Since the structure is separated into two elements,

$$\delta_c \neq \delta_d$$

$$\beta_c \neq \beta_d \quad .$$

Consequently, there exists the discontinuity as follows:

(a) in displacement $\quad \delta_c - \delta_d$

(b) in slope $\quad \beta_c - \beta_d$.

To close this gap, unknown forces (Q and M) will be introduced around the juncture to hold the two pieces together.

Displacements and rotation of the cylinder due to unit values of Q and M are defined as follows:

$$Q_c^{\delta},\ Q_c^{\beta} \text{ and } M_c^{\delta},\ M_c^{\beta} \quad .$$

The corresponding values for the dome for the same unit loadings will be:

$$Q_d^{\delta},\ Q_d^{\beta} \text{ and } M_d^{\delta},\ M_d^{\beta} \quad .$$

These unit deformations and unit loadings at the junctions are presented in Figure B7.3.2-3.

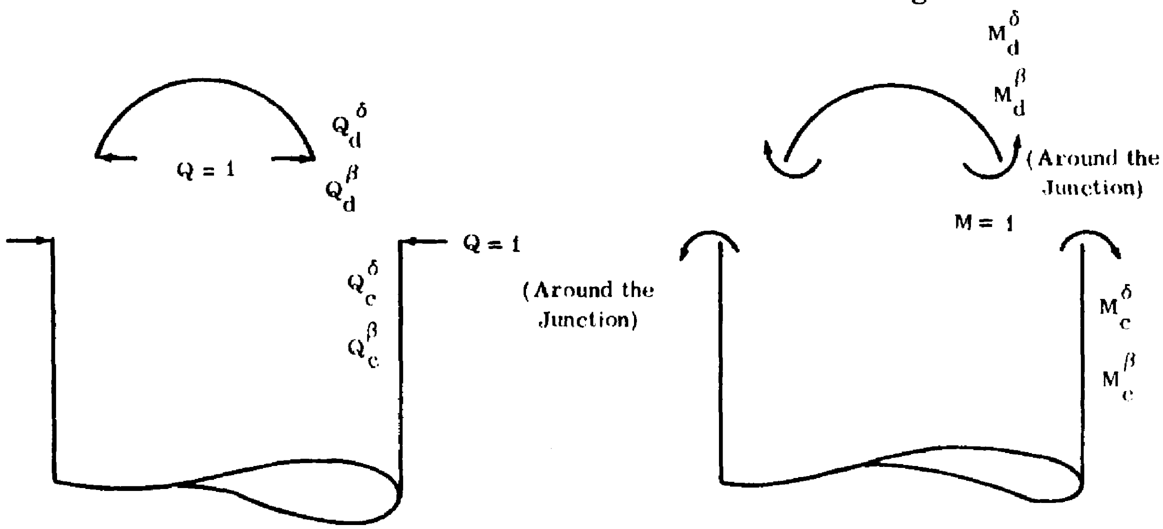

FIGURE B7. 3. 2-3 UNIT DEFORMATIONS AND UNIT LOADINGS

To close the gap, the following equations can be written:

$$\left(Q_c^\delta + Q_d^\delta\right)Q + \left(M_c^\delta + M_d^\delta\right)M = \delta_c - \delta_d$$

$$\left(Q_c^\beta + Q_d^\beta\right)Q + \left(M_c^\beta + M_d^\beta\right)M = \beta_c - \beta_d \quad .$$

Thus, with the two equations, the two unknowns (Q and M) can be determined.

It is noted that one cut through the shell leads to two algebraic equations with two unknowns.

The following sign convention is adopted:

1. Horizontal deflection, δ , is positive outward

2. Shears are positive if they cause deflection outward

3. Moments are positive if they cause tension on the inside fibers of the shell

4. Rotations are positive if they correspond to a positive moment.

In general, this sign convention is arbitrary. Any rule of signs may be adopted if it does not conflict with logic and is used consistently.

Observe that in addition to M and Q, there is an axial force distribution around the junction between the cylinder and dome (reaction of bulkhead), but the effect of this force on the displacement due to M and Q is negligible.

B7. 3. 2. 2 Interaction Between Three or More Shell Elements

In practice, most cases are similar to the two-member interaction described in the previous paragraph. However, at times it may be convenient to consider interaction of more than two elements. This can be performed in two ways:

1. Interact first the two elements; then, when this combination is solved, interact it with the third element, etc.

2. Simultaneously interact all elements.

The first method is self-explanatory. The second method requires further explanation. If the shape of the bulkhead is such that its meridian cannot be approximated with one definite analytical curve, such a bulkhead is called a compound bulkhead and can be approximated with many curves as shown in Figure B7. 3. 2-1.

In this case, two or more imaginary cuts through the shell will be required to separate the compound bulkhead into component shells of basic shape. This is shown in Figure B7. 3. 2-4, where the compound shell has two imaginary cuts separating the three elementary shells (spherical, toroidal, and cylindrical). Figure B7. 3. 2-4 also illustrates the loading and discontinuity influences that belong to each cut. The discontinuity influences will restore the continuity of the compound shell.

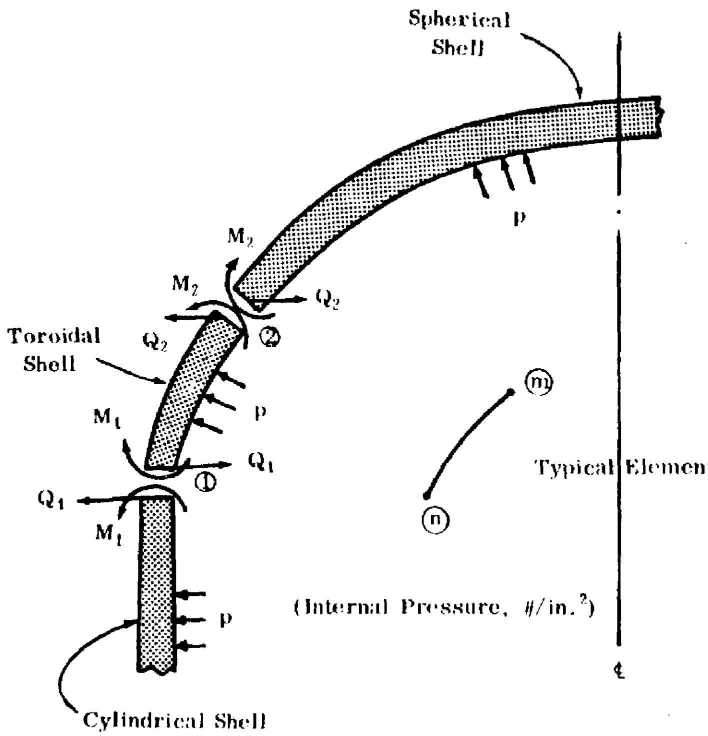

FIGURE B7. 3. 2-4 DISCONTINUITY LOADS

The symbols used for the two successive cuts m and n are also shown in Figure B7. 3. 2-4.

M_{nn}^{β}, Q_{nn}^{β} = rotation at point n due to a unit moment M or unit horizontal shear Q at point n

M_{nn}^{δ}, Q_{nn}^{δ} = horizontal displacement due to the same loading in application points as above

M_{nm}^{β}, Q_{nm}^{β} = rotation at point n due to a unit moment M or unit horizontal shear Q acting at point m

M_{nm}^{δ}, Q_{nm}^{δ} = horizontal displacement due to the same loading in application points as above.

Designating n = 1 and m = 2, the nomenclature above can be considered proper indices for the toroidal portion (1) and (2) as shown in Figure B7.3.2-4.

Additional nomenclature needed to cover the spherical shell portion of Figure B7.3.2-4 is as follows:

M_s^{β}, Q_s^{β} = rotations at point (2) on the spherical shell due to a unit moment or unit shear at the same point

M_s^{δ}, Q_s^{δ} = horizontal displacements due to the same conditions as stated above.

Similarly, displacements and rotations of point (1) on the cylindrical shell are defined by using subscript c (cylinder) instead of subscript s (sphere).

Due to the primary loading (internal pressure), the rotations and displacements will be indicated with β and $\Delta r = \Delta$. As before, the subscripts c and s refer to the cylinder and sphere. The subscripts 1t and 2t will be used to denote the toroidal shell at the edges (1) and (2).

Now the equations for the total rotation and displacement can be formed.

Spherical Shell:

$$\delta_s = M_s^{\delta} M_2 + Q_s^{\delta} Q_2 + \Delta_s p$$

$$\beta_s = M_s^{\beta} M_2 + Q_s^{\beta} Q_2 + \beta_s p$$

Toroidal Shell:

$$\delta_{2t} = M_{22}^{\delta} M_2 + Q_{22}^{\delta} Q_2 + M_{21}^{\delta} M_1 + Q_{21}^{\delta} Q_1 + \Delta_{2t} p$$

$$\beta_{2t} = M_{22}^{\beta} M_2 + Q_{22}^{\beta} Q_2 + M_{21}^{\beta} M_1 + Q_{21}^{\beta} Q_1 + \beta_{2t} p$$

$$\delta_{1t} = M_{12}^{\delta} M_2 + Q_{12}^{\delta} Q_2 + M_{11}^{\delta} M_1 + Q_{11}^{\delta} Q_1 + \Delta_{1t} p$$

$$\beta_{1t} = M_{12}^{\beta} M_2 + Q_{12}^{\beta} Q_2 + M_{11}^{\beta} M_1 + Q_{11}^{\beta} Q_1 + \beta_{1t} p$$

Cylindrical Shell:

$$\delta_c = M_c^{\delta} M_1 + Q_c^{\delta} Q_1 + \Delta_c p$$

$$\beta_c = M_c^{\beta} M_1 + Q_c^{\beta} Q_1 + \beta_c p$$

The following compatibility equations must be satisfied:

$$\delta_s = \delta_{2t} \qquad \beta_s = \beta_{2t}$$

$$\delta_c = \delta_{1t} \qquad \beta_c = \beta_{1t} \quad .$$

Following considerations of the relations above and some mathematical rearrangements, a system of four linear equations with four unknowns will finally be obtained. In matrix form they are:

$$\begin{bmatrix} M_{21}^{\delta} & \left(M_{22}^{\delta} - M_s^{\delta}\right) & Q_{21}^{\delta} & \left(Q_{22}^{\delta} - Q_s^{\delta}\right) \\ \left(M_{11}^{\delta} - M_c^{\delta}\right) & M_{12}^{\delta} & \left(Q_{11}^{\delta} - Q_c^{\delta}\right) & Q_{12}^{\delta} \\ M_{21}^{\beta} & \left(M_{22}^{\beta} - M_s^{\beta}\right) & Q_{21}^{\beta} & \left(Q_{22}^{\beta} - Q_s^{\beta}\right) \\ \left(M_{11}^{\beta} - M_c^{\beta}\right) & M_{12}^{\beta} & \left(Q_{11}^{\beta} - Q_c^{\beta}\right) & Q_{12}^{\beta} \end{bmatrix} \begin{bmatrix} M_1 \\ M_2 \\ Q_1 \\ Q_2 \end{bmatrix} + \begin{bmatrix} \Delta_{2t} - \Delta_s \\ \Delta_{1t} - \Delta_c \\ \beta_{2t} - \beta_s \\ \beta_{1t} - \beta_c \end{bmatrix} p = 0 \quad .$$

It is noted that two imaginary cuts lead to four equations with four unknowns: M_1, M_2, Q_1, and Q_2.

Previously, when considering only one imaginary cut, only two equations with two unknowns were obtained. Consequently, if n imaginary cuts are introduced simultaneously, 2n linear equations with 2n unknowns can be obtained.

It can be concluded that the problem of interaction is reduced to the problem of finding rotation (β) and displacements ($\Delta r = \delta$) of interacting structural elements due to the primary loadings and the secondary loadings ($M = Q = 1$) (around the junction). The rotations and displacements then will be introduced into a set of linear equations and statically indeterminate values (M and Q) will be found.

B7.3.3 EDGE INFLUENCE COEFFICIENTS

The shells considered in this section are homogeneous isotropic monocoque shells of revolution. Thin shells are considered and all loadings are axisymmetrical. Paragraph B7.3.4 will present necessary modifications of derived formulas for nonhomogeneous material and nonmonocoque shells.

B7.3.3.1 General Discussion

Unit loadings (defined in Paragraph B7.3.1.2) are the loadings acting on upper or lower edge of shell:

$M = 1$ lb-in./in.

$Q = 1$ lb/in.

Unit influences are deformations and forces in a shell of revolution due to unit loadings. Influences of this nature are of load character and do not progress very far into the shell from the disturbed edge. Various differently shaped shells are covered at this location. Of special interest is a shell that represents a bulkhead, which is characterized with $\phi_{max} = 90°$; such bulkheads are very common in aerospace vehicles and pressure vessels. The bulkhead shells are tangent to the cylindrical body of the vehicle.

When the values of deformations due to the unit loadings are available, the deformations, along with the primary deformations, can be used to determine discontinuity stresses (Paragraph B7.3.2).

The bending theory is used to obtain the influence coefficients due to unit loadings. The fundamentals of this procedure were explained previously.

It has been mentioned that deflections and internal loads due to unit loadings are of local importance. It can be concluded that disturbances due to edge-unit loadings will disappear completely for $\alpha \geqq 20°$ and will become negligible for $\alpha \geqq 10°$, as shown in Table B7.3.3-1, for a spherical shell.

TABLE B7.3.3-1 UNIT-EDGE LOADING SOLUTIONS

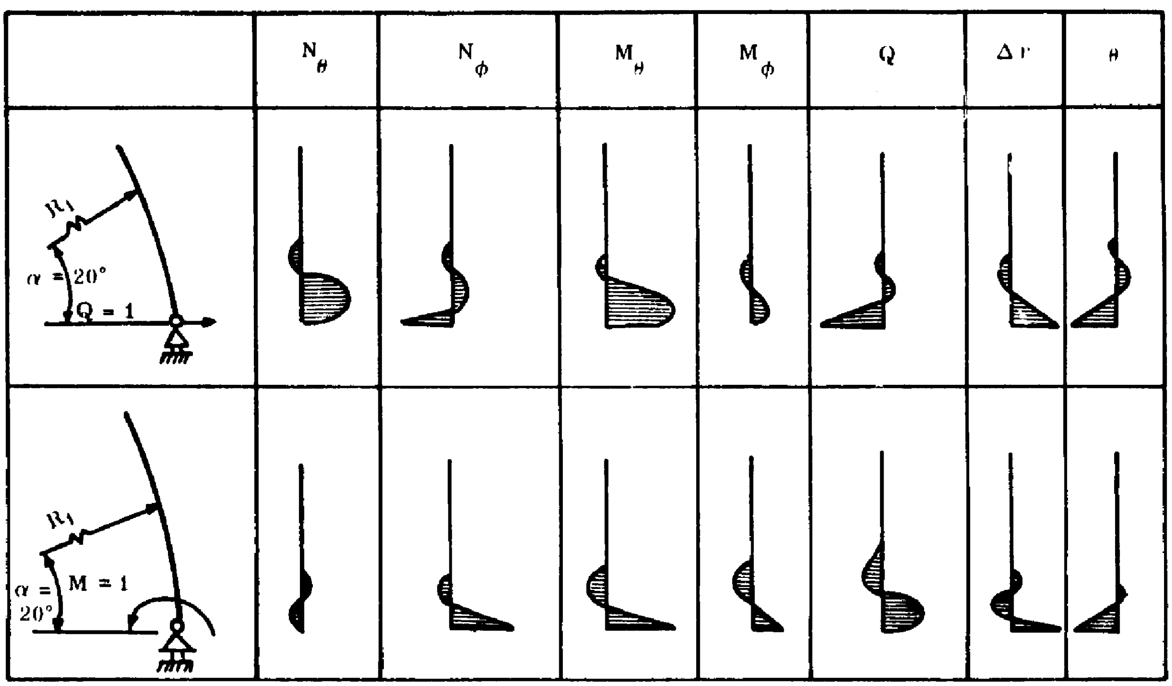

Table B7.3.3-1 illustrates a very important conclusion: due to the unit-edge loadings, practically all parts of the shell satisfying the condition $\alpha \geq 20°$ will remain unstressed and undisturbed. These parts will not be needed for satisfying equilibrium. They do not affect the stresses and deformations in the disturbed zone $0 < \alpha < 20°$ in any way. The material above $\alpha = 20°$ can be deleted because this material does not contribute to the stresses or strains, which are computed for the zone defined by $0 < \alpha < 20°$. No values of stresses or deformations will be changed in the zone $0 < \alpha < 20°$ if we replace the removed material with any shape of shell (Figure B7.3.3-1) which illustrates imaginary operations. Consequently, cases (A), (B), and (C) of Figure B7.3.3-1 are statically equivalent. This discussion leads to the following conclusions:

1. The spherical shell of revolution, loaded with the unit loadings ($M = Q = 1$), acts as a lower segment would act under the same loading (segment defined with $\alpha = 20°$). Consequently, it does not matter what shape the rest of the shell has (Figure B7.3.3-2).

2. If any shell at the lower portion (which is adjusted to the load edge) can be approximated with the spherical shell to a satisfactory degree, the solution obtained for the spherical shell which is loaded with $M = Q = 1$ all around the edges (Figures B7.3.3-2 and B7.3.3-3) can be used for the actual shell.

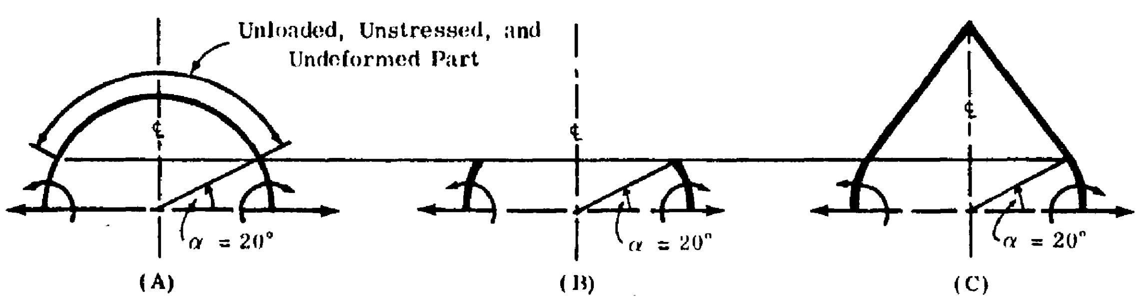

FIGURE B7.3.3-1 STATICALLY ANALOGICAL SHELLS

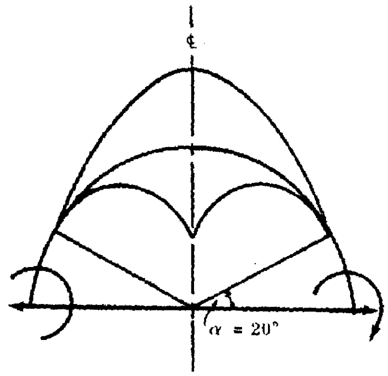

FIGURE B7.3.3-2 DIFFERENT VARIANTS FOR UNSTRESSED PORTION

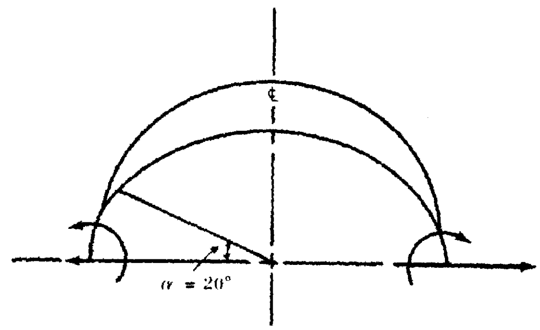

FIGURE B7.3.3-3 APPROXIMATION WITH THE SPHERE

3. When accuracy requirements are relaxed, $\alpha = 10^\circ$ may be used in place of $\alpha = 20^\circ$.

Another approximation, known as Geckeler's assumption, may be useful; i.e., if the thickness of the shell (t) is small in comparison with equatorial radius ($r_1 = a$) and limited by the relation ($a/t > 50$), the bending stresses at the edge may be determined by cylindrical shell theory. Meissner even recommends $a/t > 30$. This means that the bulkhead shell can be approximated with a cylinder for finding unit influences. Many solutions can be presented for various shaped shells due to the unit loading action. This is done in the following paragraphs.

B7.3.3.2 Definition of F-Factors

The general solution of the homogeneous differential equation

$$w'''' + 4K^4 w = 0$$

can be represented with the following combination of trigonometric and hyperbolic functions:

$\cosh kL\xi \cos kL\xi$ $\qquad$ $\sinh kL\xi \cos kL\xi$

$\cosh kL\xi \sin kL\xi$ $\qquad$ $\sinh kL\xi \sin kL\xi$

where kL is a dimensionless parameter and ξ is a dimensionless ordinate.

In the sections which follow, F-factors will be used that simplify the analysis. Definitions of the F-factors in Table B7.3.3-2 are taken from Reference 2. As a special parameter for determining the F-factors, η is considered as follows:

$$F = F(\eta) \quad \text{i.e.,} \quad F_1 = \sinh^2\eta + \sin^2\eta$$

For a cylindrical shell

$$\eta = kL \text{ or } \eta = kL\xi \text{ and } k = \frac{\sqrt[4]{3(1-\mu^2)}}{\sqrt{Rt}}$$

For a conical shell

$$\eta = kL \text{ or } \eta = kL \text{ and } k = \frac{\sqrt[4]{3(1-\mu^2)}}{\sqrt{tx_m \cot\alpha_0}}$$

For a spherical shell

$$\eta = k \text{ for } F_i;\ \eta = k\alpha \text{ for } F_i(\alpha) \text{ and } k = \sqrt[4]{3(1-\mu^2)\ (R/t)^2} \quad .$$

Graphs of the functions are presented in Reference 2.

TABLE B7.3.3-2 $F_i(\xi)$ AND F_i FACTORS

i	$F_i(\xi)$	F_i
1	$\sinh^2 kL\xi - \sin^2 kL\xi$	$\sinh^2 kL - \sin^2 kL$
2	$\sinh^2 kL\xi + \sin^2 kL\xi$	$\sinh^2 kL + \sin^2 kL$
3	$\sinh kL\xi \cosh kL\xi + \sin kL\xi \cos kL\xi$	$\sinh kL \cosh kL + \sin kL \cos kL$
4	$\sinh kL\xi \cosh kL\xi - \sin kL\xi \cos kL\xi$	$\sinh kL \cosh kL - \sin kL \cos kL$
5	$\sin^2 kL\xi$	$\sin^2 kL$
6	$\sinh^2 kL\xi$	$\sinh^2 kL$
7	$\cosh kL\xi \cos kL\xi$	$\cosh kL \cos kL$
8	$\sinh kL\xi \sin kL\xi$	$\sinh kL \sin kL$
9	$\cosh kL\xi \sin kL\xi - \sinh kL\xi \cos kL\xi$	$\cosh kL \sin kL - \sinh kL \cos kL$
10	$\cosh kL\xi \sin kL\xi + \sinh kL\xi \cos kL\xi$	$\cosh kL \sin kL + \sinh kL \cos kL$
11	$\sin kL\xi \cos kL\xi$	$\sin kL \cos kL$
12	$\sinh kL\xi \cosh kL\xi$	$\sinh kL \cosh kL$
13	$\cosh kL\xi \cos kL\xi - \sinh kL\xi \sin kL\xi$	$\cosh kL \cos kL - \sinh kL \sin kL$
14	$\cosh kL\xi \cos kL\xi + \sinh kL\xi \sin kL\xi$	$\cosh kL \cos kL + \sinh kL \sin kL$
15	$\cosh kL\xi \sin kL\xi$	$\cosh kL \sin kL$
16	$\sinh kL\xi \cos kL\xi$	$\sinh kL \cos kL$
17	$\exp(-kL\xi \cos kL\xi)$	$\exp(-kL \cos kL)$
18	$\exp(-kL\xi \sin kL\xi)$	$\exp(-kL \sin kL)$
19	$\exp[-kL\xi(\cos kL\xi + \sin kL\xi)]$	$\exp[-kL(\cos kL + \sin kL)]$
20	$\exp[-kL\xi(\cos kL\xi - \sin kL\xi)]$	$\exp[-kL(\cos kL - \sin kL)]$

B7.3.3.3 Spherical Shells

The boundaries of the shells considered herein must be free to rotate and deflect vertically and horizontally because of the action of unit loadings. Abrupt discontinuities in the shell thickness must not be present. Thickness of the shell must be uniform in the range in which the stresses exist.

I Nonshallow Spherical Shells

Formulas will be tabulated for closed and open spherical shells. Open shells are shells that have an axisymmetrical circular opening at the apex. Unit-edge loadings may act at the lower or upper edge of the open shell. Linear bending theory was employed for derivation of the formulas presented.

The following designations will be used:

$$k = \sqrt[4]{(R/t)^2\, 3(1-\mu^2)}\ ;\ \alpha = \phi_1 - \phi\quad .$$

Tables B7.3.3-3, B7.3.3-4, B7.3.3-5, and B7.3.3-6 are presented.

II Shallow Spherical Shells

This section presents, for shallow spherical shells, the solutions which satisfy the relation

$$\cot\phi \cong \frac{1}{\phi}$$

which is characteristic for the category of shallow spherical shells. Physically, this means that for shallow shells the disturbances resulting from unit-edge loadings will not decay before reaching the apex. Consequently, from diametrically opposite edge loadings, disturbances will be superimposed in some area around the apex.

Tables B7.3.3-7 and B7.3.3-8 are presented.

TABLE B7. 3. 3-3 CLOSED SPHERICAL SHELL

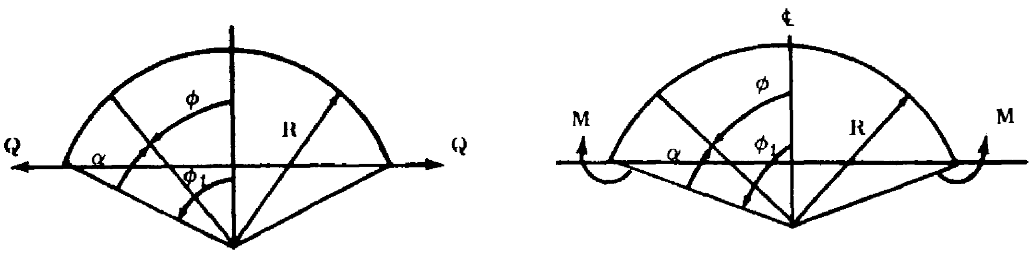

Q_ϕ	$-\sqrt{2}Q \sin\phi_1 e^{-k\alpha} \cos\left(k\alpha + \frac{\pi}{4}\right)$	$+\frac{2Mk}{R} e^{-k\alpha} \sin k\alpha$
N_ϕ	$-Q_\phi \cot\phi$	$-Q_\phi \cot\phi$
N_θ	$2Qk \sin\phi_1 e^{-k\alpha} \cos k\alpha$	$2\sqrt{2}\ \frac{Mk^2}{R} e^{-k\alpha} \cos\left(k\alpha + \frac{\pi}{4}\right)$
M_ϕ	$\frac{RQ}{k} \sin\phi_1 e^{-k\alpha} \sin k\alpha$	$\sqrt{2}Me^{-k\alpha} \sin\left(k\alpha + \frac{\pi}{4}\right)$
M_θ	$-\frac{RQ}{k^2\sqrt{2}} \sin\phi_1(\cot\phi) e^{-k\alpha}$ $\sin\left(k\alpha + \frac{\pi}{4}\right) + \mu M_\phi$	$\frac{M}{k} \cot\phi\ e^{-k\alpha} \cos k\alpha + \mu M_\phi$
$Et\beta$	$-2\sqrt{2}Qk^2 \sin\phi_1 e^{-k\alpha} \sin\left(k\alpha + \frac{\pi}{4}\right)$	$-\frac{4k^3M}{R} e^{-k\alpha} \cos k\alpha$
$Et(\Delta r)$	$RQ \sin\phi_1 e^{-k\alpha}\left[2k \sin\phi \cos k\alpha - \sqrt{2}\mu\right.$ $\left.\cos\phi \cos\left(k\alpha + \frac{\pi}{4}\right)\right]$	$R \sin\phi\left(N_\theta - \mu N_\phi\right)$
For $\alpha = 0,\ \phi = \phi_1$		
$Et\beta$	$-2Qk^2 \sin\phi_1$	$-\frac{4k^3M}{R}$
$Et(\Delta r)$	$QR \sin\phi_1\left(2k \sin\phi_1 - \mu\cos\phi_1\right)$	$2Mk^2 \sin\phi_1$
For $\phi_1 = 90°,\ \alpha = 0$		
$Et\beta$	$-2k^2Q$	$-\frac{4k^3}{R} M$
$Et(\Delta r)$	$2RkQ$	$2k^2M$

TABLE B7. 3. 3-4 OPEN SPHERICAL SHELL

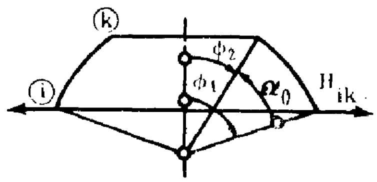

Boundary Conditions

$\alpha = 0(\phi = \phi_1)$: $M_\phi = 0$ $H_{ik} = Q_{ik} \sin \phi_1 + N_{ik} \cos \phi_1$ $\alpha = \alpha_0(\phi = \phi_2)$ $M_\phi = 0$ $Q = 0$

Internal Forces and Deformations

N_ϕ	$H_{ik} \sin \phi \cot \phi \left[F_7(\alpha) - \frac{F_4}{F_1} F_{10}(\alpha) + \frac{F_2}{F_1} F_8(\alpha)\right]$
N_θ	$-H_{ik} k \sin \phi_1 \left[-F_9(\alpha) - 2 \frac{F_4}{F_1} F_7(\alpha) + \frac{F_2}{F_1} F_{10}(\alpha)\right]$
Q_ϕ	$H_{ik} \sin \phi_1 \left[F_7(\alpha) - \frac{F_4}{F_1} F_{10}(\alpha) + \frac{F_2}{F_1} F_8(\alpha)\right]$
M_ϕ	$-H_{ik} \frac{R}{2k} \sin \phi_1 \left[-F_{10}(\alpha) + 2 \frac{F_4}{F_1} F_8(\alpha) - \frac{F_2}{F_1} F_9(\alpha)\right]$
M_θ	$H_{ik} \frac{R}{2k} \sin \phi_1 \left\{ -\left[\frac{\cot \phi}{k} F_8(\alpha) - \mu F_{10}(\alpha)\right] + \frac{F_4}{F_1}\left[\frac{\cot \phi}{k} F_9(\alpha) - 2\mu F_8(\alpha)\right] + \frac{F_2}{F_1}\left[\frac{\cot \phi}{k} F_7(\alpha) + \mu F_9(\alpha)\right] \right\}$
Δr	$-H_{ik} \frac{Rk}{Et} \sin \phi \sin \phi_1 \left[-F_9(\alpha) - 2 \frac{F_4}{F_1} F_7(\alpha) + \frac{F_2}{F_1} F_{10}(\alpha)\right]$
β	$-H_{ik} \frac{2k^2}{Et} \sin \phi_1 \left[-F_8(\alpha) - \frac{F_4}{F_1} F_9(\alpha) + \frac{F_2}{F_1} F_7(\alpha)\right]$

TABLE B7.3.3-4 OPEN SPHERICAL SHELL (Continued)

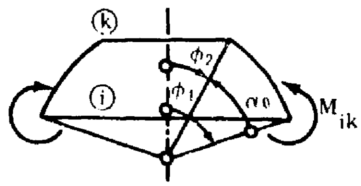

Boundary Conditions

$\alpha = 0$	$M_\phi = -M_{ik}$
	$Q_\phi = 0$
$\alpha = \alpha_0$	$M_\phi = 0$
	$Q_\phi = 0$

Internal Forces and Deformations

N_ϕ	$M_{ik} \cot\phi \, \frac{2k}{R}\left[\frac{F_6}{F_1} F_{15}(\alpha) + \frac{F_5}{F_1} F_{16}(\alpha) - \frac{F_3}{F_1} F_8(\alpha)\right]$
N_θ	$-M_{ik} \frac{2K^2}{R}\left[\frac{F_6}{F_1} F_{14}(\alpha) + \frac{F_5}{F_1} F_{13}(\alpha) - \frac{F_3}{F_1} F_{10}(\alpha)\right]$
Q_ϕ	$M_{ik} \frac{2k}{R}\left[\frac{F_6}{F_1} F_{15}(\alpha) + \frac{F_5}{F_1} F_{16}(\alpha) - \frac{F_3}{F_1} F_8(\alpha)\right]$
M_ϕ	$M_{ik}\left\{\frac{F_6}{F_1}\left[\frac{\cot\phi}{k} F_{16}(\alpha) - \mu F_{13}(\alpha)\right] - \frac{F_5}{F_1}\left[\frac{\cot\phi}{k} F_{15}(\alpha) - \mu F_{14}(\alpha)\right] - \frac{F_3}{F_1}\left[\frac{\cot\phi}{k} F_7(\alpha) + \mu F_9(\alpha)\right]\right\}$
M_θ	$-M_{ik}\left[\frac{F_6}{F_1} F_{13}(\alpha) - \frac{F_5}{F_1} F_{14}(\alpha) + \frac{F_3}{F_1} F_9(\alpha)\right]$
Δr	$-M_{ik} \frac{2k^2}{Et} \sin\phi \left[\frac{F_6}{F_1} F_{14}(\alpha) + \frac{F_5}{F_1} F_{13}(\alpha) - \frac{F_3}{F_1} F_{10}(\alpha)\right]$
β	$-M_{ik} \frac{4k^3}{EtR}\left[\frac{F_6}{F_1} F_{16}(\alpha) - \frac{F_5}{F_1} F_{15}(\alpha) - \frac{F_3}{F_1} F_7(\alpha)\right]$

TABLE B7. 3. 3-4 OPEN SPHERICAL SHELL (Continued)

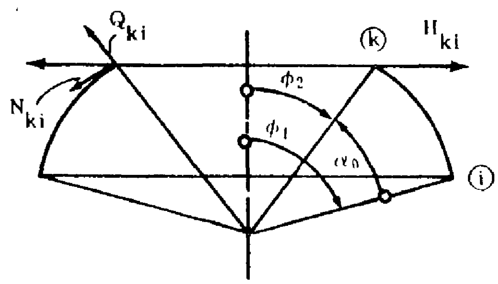

Boundary Conditions

$\alpha = 0 (\phi = \phi_1)$	$M_\phi = 0$	
	$Q_\phi = 0$	
$\alpha = \alpha_0 (\phi = \phi_2)$	$M_\phi = 0$	
	$H_{ki} = -Q_{ki} \sin \phi_2 - N_{ki} \cos \phi_2$	

Internal Forces and Deformations

N_ϕ	$H_{ki} \cot \phi \sin \phi_2 \left[\frac{F_9}{F_1} F_{10}(\alpha) - 2 \frac{F_8}{F_1} F_8(\alpha) \right]$
N_θ	$H_{ki}\, 2k \sin \phi_2 \left[- \frac{F_9}{F_1} F_7(\alpha) + \frac{F_8}{F_1} F_{10}(\alpha) \right]$
Q_ϕ	$H_{ki} \sin \phi_2 \left[\frac{F_9}{F_1} F_{10}(\alpha) - \frac{2F_8}{F_1} F_8(\alpha) \right]$
M_ϕ	$H_{ki} \frac{R}{k} \sin \phi_2 \left[\frac{F_9}{F_1} F_8(\alpha) - \frac{F_8}{F_1} F_9(\alpha) \right]$
M_θ	$H_{ki} \frac{R}{2k} \sin \phi_2 \left\{ \frac{F_9}{F_1} \left[- \frac{\cot \phi}{k} F_9(\alpha) + \mu 2 F_8(\alpha) \right] - \frac{2F_8}{F_1} \left[\frac{\cot \phi}{k} F_7(\alpha) + \mu F_9(\alpha) \right] \right\}$
Δr	$-H_{ki} \sin \phi_2 \frac{Rk}{Et} 2 \sin \phi \left[\frac{F_9}{F_1} F_7(\alpha) - \frac{F_8}{F_1} F_{10}(\alpha) \right]$
β	$H_{ki} \sin \phi_2 \frac{2k^2}{Et} \left[\frac{F_9}{F_1} F_9(\alpha) + \frac{2F_8}{F_1} F_7(\alpha) \right]$

TABLE B7.3.3-4 OPEN SPHERICAL SHELL (Concluded)

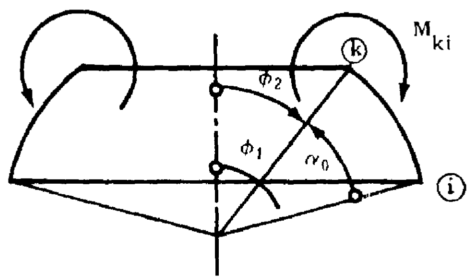

Boundary Conditions

$\alpha = 0(\phi = \phi_1)$: $M_\phi = 0$

$Q_\phi = 0$

$\alpha = \alpha_0(\phi = \phi_2)$: $M_\phi = M_{ki}$

$Q_\phi = 0$

Internal Forces and Deformations

N_ϕ	$M_{ki}\,\frac{2k}{R}\,\cot\phi\left[\frac{F_8}{F_1}\,F_{10}(\alpha) - \frac{F_{10}}{F_1}\,F_8(\alpha)\right]$
N_θ	$M_{ki}\,\frac{2k^2}{R}\left[-2\,\frac{F_8}{F_1}\,F_7(\alpha) + \frac{F_{10}}{F_1}\,F_{10}(\alpha)\right]$
Q_ϕ	$-M_{ki}\,\frac{2k}{R}\left[-\frac{F_8}{F_1}\,F_{10}(\alpha) + \frac{F_{10}}{F_1}\,F_8(\alpha)\right]$
M_ϕ	$M_{ki}\left[2\,\frac{F_8}{F_1}\,F_8(\alpha) - \frac{F_{10}}{F_1}\,F_9(\alpha)\right]$
M_θ	$-M_{ki}\left\{\frac{F_8}{F_1}\left[\frac{\cot\phi}{k}\,F_9(\alpha) - \mu 2F_8(\alpha)\right] + \frac{F_{10}}{F_1}\left[\frac{\cot\phi}{k}\,F_7(\alpha) + F_7(\alpha)\right]\right\}$
Δr	$M_{ki}\,\frac{2k^2}{Et}\,\sin\phi\left[-2\,\frac{F_8}{F_1}\,F_7(\alpha) + \frac{F_{10}}{F_1}\,F_{10}(\alpha)\right]$
β	$M_{ki}\,\frac{4k^3}{EtR}\left[\frac{F_8}{F_1}\,F_9(\alpha) + \frac{F_{10}}{F_1}\,F_7(\alpha)\right]$

TABLE B7.3.3-5 SPHERICAL SEGMENT WITH FREE EDGES, EDGE DISTORTIONS RESULTING FROM SECONDARY LOADINGS

Edge Distortions / Loading Condition	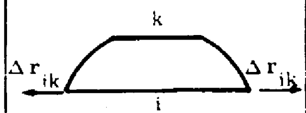	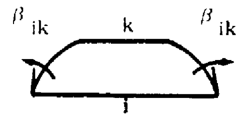	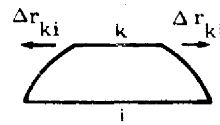	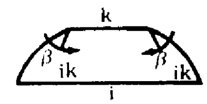
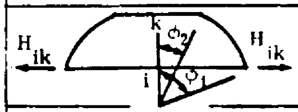	$+H_{ik}\frac{2Rk}{Et}\sin^2\phi_1\frac{F_4}{F_1}$	$-H_{ik}\frac{2k^2}{Et}\sin\phi_1\frac{F_2}{F_1}$	$-H_{ik}\frac{2Rk}{Et}\sin\phi_1\sin\phi_2\frac{F_9}{F_1}$	$-H_{ik}\frac{2k^2}{Et}\sin\phi_1\frac{2F_8}{F_1}$
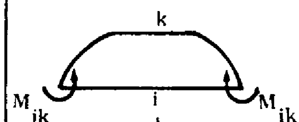	$-M_{ik}\frac{2k^2}{Et}\sin\phi_1\frac{F_{[illegible]}}{F_1}$	$-M_{ik}\frac{2k^3}{EtR}\frac{2F_3}{F_1}$	$-M_{ik}\frac{2k^2}{Et}\sin\phi_2\frac{2F_8}{F_1}$	$+M_{ik}\frac{2k^3}{EtR}\frac{2F_{10}}{F_1}$
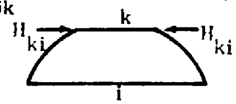	$-H_{ki}\frac{2Rk}{Et}\sin\phi_1\sin\phi_2\frac{F_{[illegible]}}{F_1}$	$-H_{ki}\frac{2k^2}{Et}\sin\phi_2\frac{2F_8}{F_1}$	$-H_{ki}\frac{2Rk}{Et}\sin^2\phi_2\frac{F_4}{F_1}$	$-H_{ki}\frac{2k^2}{Et}\sin\phi_2\frac{F_2}{F_1}$
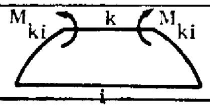	$-M_{ki}\frac{2k^2}{Et}\sin\phi_1\frac{2F_3}{F_1}$	$-M_{ki}\frac{2k^3}{EtR}\frac{2F_{10}}{F_1}$	$-M_{ki}\frac{2k^2}{Et}\sin\phi_2\frac{F_{[illegible]}}{F_1}$	$+M_{ki}\frac{2k^3}{EtR}\frac{2F_3}{F_1}$

TABLE B7. 3. 3-6 OPEN (OR CLOSED) SPHERICAL SHELL EXPOSED TO UNIT DISTORTIONS AT LOWER EDGE

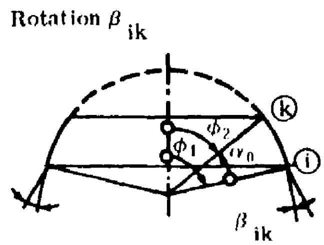

Boundary Conditions

$\alpha = 0(\phi = \phi_1)$: $\Delta r = 0 : \beta = \beta_{ik}$
$\alpha = \alpha_0(\phi = \phi_2)$: $\Delta r = 0 : \beta = 0$

Internal Forces and Deformations

N_ϕ	$\beta_{ik} \cot\phi \dfrac{Et}{2k^2}\left[\dfrac{F_2}{F_1}F_7(\alpha) + \dfrac{F_4}{F_1}F_9(\alpha) - F_8(\alpha)\right]$
N_θ	$-\beta_{ik}\dfrac{Et}{2k}\left[-\dfrac{F_2}{F_1}F_9(\alpha) + 2\dfrac{F_4}{F_1}F_8(\alpha) - F_{10}(\alpha)\right]$
Q_ϕ	$\beta_{ik}\dfrac{Et}{2k^2}\left[\dfrac{F_2}{F_1}F_7(\alpha) + \dfrac{F_4}{F_1}F_9(\alpha) - F_8(\alpha)\right]$
M_ϕ	$-\beta_{ik}\dfrac{R\,Et}{4k^3}\left[-\dfrac{F_2}{F_1}F_{10}(\alpha) + 2\dfrac{F_4}{F_1}F_7(\alpha) + F_9(\alpha)\right]$
M_θ	$\beta_{ik}\dfrac{R\,Et}{4k^3}\left\{-\dfrac{F_2}{F_1}\left[\dfrac{\cot\phi}{k}F_8(\alpha) - \mu F_{10}(\alpha)\right] + \dfrac{F_4}{F_1}\left[\dfrac{\cot\phi}{k}F_{10}(\alpha) - 2\mu F_7(\alpha)\right] - \left[\dfrac{\cot\phi}{k}F_7(\alpha) + \mu F_9(\alpha)\right]\right\}$
Δr	$-\beta_{ik}\dfrac{R}{2k}\sin\phi\left[-\dfrac{F_2}{F_1}F_9(\alpha) + 2\dfrac{F_4}{F_1}F_8(\alpha) - F_{10}(\alpha)\right]$
β	$-\beta_{ik}\left[-\dfrac{F_2}{F_1}F_8(\alpha) + \dfrac{F_4}{F_1}F_{10}(\alpha) - F_7(\alpha)\right]$

TABLE B7.3.3-6 OPEN (OR CLOSED) SPHERICAL SHELL EXPOSED TO UNIT DISTORTIONS AT LOWER EDGE (Continued)

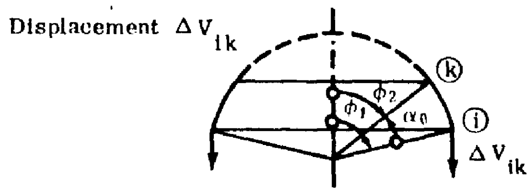

Boundary Conditions

$\alpha = (\phi = \phi_1)$: $\beta = 0$, $\Delta V = \Delta V_{ik}$

$\alpha = \alpha_0(\phi = \phi_2)$: $\beta = 0$, $\Delta V = 0$

Internal Forces and Deformations

N_ϕ	$\frac{\Delta V_{ik} Et \cot\phi}{R[(1+\mu)\sin\phi_1 F_3 + k\cos\phi_1 F_1]}[-F_3F_7(\alpha) - F_5F_{15}(\alpha) + F_6F_{16}(\alpha)]$
N_θ	$\frac{-\Delta V_{ik} Et\, k}{R[(1+\mu)\sin\phi_1 F_3 + k\cos\phi_1 F_1]}[F_3F_9(\alpha) - F_5F_{14}(\alpha) + F_6F_{13}(\alpha)]$
Q_ϕ	$\frac{\Delta V_{ik} Et}{R[(1+\mu)\sin\phi_1 F_3 + k\cos\phi_1 F_1]}[-F_3F_7(\alpha) - F_5F_{15}(\alpha) + F_6F_{16}(\alpha)]$
M_ϕ	$\frac{-\Delta V_{ik} Et}{2k[(1+\mu)\sin\phi_1 F_3 + k\cos\phi_1 F_1]}[F_3F_{10}(\alpha) - F_5F_{13}(\alpha) - F_6F_{14}(\alpha)]$
M_θ	$\frac{\Delta V_{ik} Et}{2k[(1+\mu)\sin\phi_1 F_3 + k\cos\phi_1 F_1]}\left\{F_3\left[\frac{\cot\phi}{k}F_8(\alpha) - \mu F_{10}(\alpha)\right] - F_5\left[\frac{\cot\phi}{k}F_{16}(\alpha) - \mu F_{13}(\alpha)\right] - F_6\left[\frac{\cot\phi}{k}F_{15}(\alpha) - \mu F_{14}(\alpha)\right]\right\}$
Δr	$\frac{-\Delta V_{ik}\, k\sin\phi}{[(1+\mu)\sin\phi_1 F_3 + k\cos\phi_1 F_1]}[F_3F_9(\alpha) - F_5F_{14}(\alpha) + F_6F_{13}(\alpha)]$
β	$\frac{2k^2\Delta V_{ik}}{R[(1+\mu)\sin\phi_1 F_3 + k\cos\phi_1 F_1]}[F_3F_8(\alpha) - F_5F_{16}(\alpha) - F_6F_{15}(\alpha)]$

TABLE B7.3.3-6 OPEN (OR CLOSED) SPHERICAL SHELL EXPOSED TO UNIT DISTORTIONS AT LOWER EDGE (Concluded)

Displacement Δr_{ik}

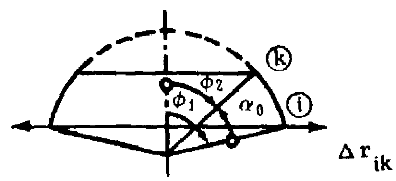

Boundary Conditions

$\alpha = 0(\phi = \phi_1): \ \Delta r = \Delta r_{ik}, \ \beta = 0$

$\alpha = 0(\phi = \phi_2): \ \Delta r = 0, \ \beta = 0$

Internal Forces and Deformations

N_ϕ	$\Delta r_{ik} \cot\phi \dfrac{Et}{Rk \sin\phi} \left[\dfrac{F_3}{F_1} F_7(\alpha) + \dfrac{F_5}{F_1} F_{15}(\alpha) - \dfrac{F_6}{F_1} F_{16}(\alpha)\right]$
N_θ	$\Delta r_{ik} \dfrac{Et}{R \sin\phi_1} \left[\dfrac{F_3}{F_1} F_9(\alpha) - \dfrac{F_5}{F_1} F_{14}(\alpha) + \dfrac{F_6}{F_1} F_{13}(\alpha)\right]$
Q_ϕ	$\Delta r_{ik} \dfrac{Et}{Rk \sin\phi_1} \left[\dfrac{F_3}{F_1} F_7(\alpha) \dfrac{F_5}{F_1} F_{15}(\alpha) - \dfrac{F_6}{F_1} F_{16}(\alpha)\right]$
M_ϕ	$\Delta r_{ik} \dfrac{Et}{2k^2 \sin\phi_1} \left[\dfrac{F_3}{F_1} F_{10}(\alpha) - \dfrac{F_5}{F_1} F_{13}(\alpha) - \dfrac{F_6}{F_1} F_{14}(\alpha)\right]$
M_θ	$\Delta r_{ik} \dfrac{Et}{2k^2 \sin\phi} \left\{ -\dfrac{F_3}{F_1} \left[\dfrac{\cot\phi}{k} F_8(\alpha) - \mu F_{10}(\alpha)\right] + \dfrac{F_5}{F_1} \left[\dfrac{\cot\phi}{k} F_{16}(\alpha) - \mu F_{13}(\alpha)\right] + \dfrac{F_6}{F_1} \left[\dfrac{\cot\phi}{k} F_{15}(\alpha) - \mu F_{14}(\alpha)\right] \right\}$
Δr	$\Delta r_{ik} \dfrac{\sin\phi}{\sin\phi_1} \left[\dfrac{F_3}{F_1} F_9(\alpha) - \dfrac{F_5}{F_1} F_{14}(\alpha) + \dfrac{F_6}{F_1} F_{13}(\alpha)\right]$
β	$\Delta r_{ik} \dfrac{2k}{R \sin\phi_1} \left[\dfrac{F_3}{F_1} F_8(\alpha) - \dfrac{F_5}{F_1} F_{16}(\alpha) - \dfrac{F_6}{F_1} F_{15}(\alpha)\right]$

TABLE B7.3.3-7 EDGE-LOADED SHALLOW SPHERICAL SHELLS

Complete (or "Long") Spherical Cap, Shallow, Constant t, Edge Moment M	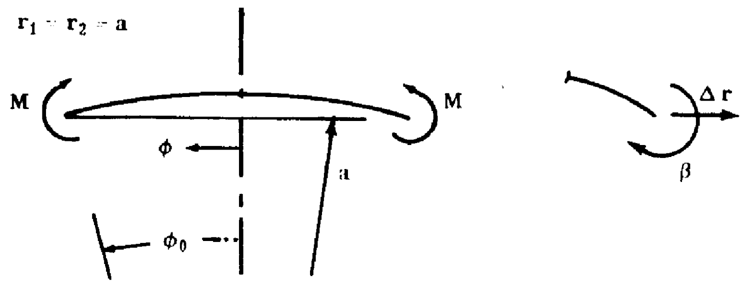
Basis	Esslinger's Approximation
Differential Equation and Boundary Conditions	$\frac{d^4Q_\phi}{d\phi^4} + \frac{2}{\phi}\frac{d^3Q_\phi}{d\phi^3} - \frac{3}{\phi^2}\frac{d^2Q_\phi}{d\phi^2} + \frac{3}{\phi^3}\frac{dQ_\phi}{d\phi} - \frac{3}{\phi^4}Q_\phi + 4k^4Q_\phi = 0$ where $k^4 = 3(1-\mu^2)\frac{a^2}{t^2}$ $Q_\phi \Big\|_{\phi=\phi_0} = 0 \qquad M_\phi \Big\|_{\phi=\phi_0} = M$
Solution	$Q_\phi = \left[\frac{C_{1M}}{k}\mathrm{Ber}'(k\sqrt{2}\phi) - \frac{C_{2M}}{k}\mathrm{Bei}'(k\sqrt{2}\phi)\right]\frac{M}{t}$
Forces	$N_\phi = (n_1 C_{1M} + n_2 C_{2M})\frac{M}{t}$ $N_\theta = (\eta_1 C_{1M} + \eta_2 C_{2M})\frac{M}{t}$ $M_\phi = (m_1 C_{1M} + m_2 C_{2M}) M$ $M_\theta = \mu M_\phi + (k_1 C_{1M} + k_2 C_{2M}) M$
Edge Influence Coefficients	$C_{VM} = -\frac{X_b}{Et^2\phi_0} \qquad C_{wM} = \frac{X_a}{Et\phi_0}$

Notes: Approximate useful range: $\phi_0 < 20°$.

For $\mathrm{Ber}'(k\sqrt{2}\phi)$, $\mathrm{Bei}'(k\sqrt{2}\phi)$ see Reference 3.

For C_{1M}, C_{2M}, X_a, and X_b as functions of $\sqrt{2}\phi_0$ see Table B7.3.3-8.

For n_1, n_2, ... etc. as function of $k\sqrt{2}\phi$ see Table B7.3.3-8

TABLE B7.3.3-7 EDGE-LOADED SHALLOW SPHERICAL SHELLS (Continued)

Complete (or "Long") Spherical Cap, Shallow, Constant t, Edge Force H	$r_1 = r_2 = a$ 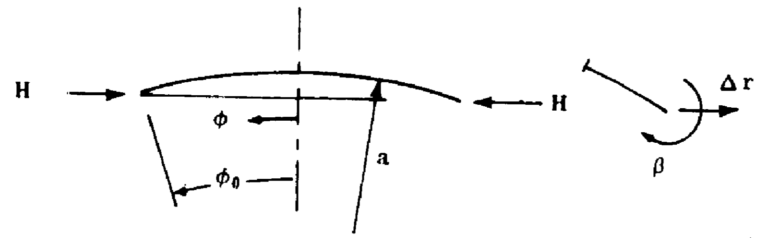
Basis	Esslinger's Approximation
Differential Equation and Boundary Conditions	$\frac{d^4Q_\phi}{d\phi^4} + \frac{2}{\phi}\frac{d^3Q_\phi}{d\phi^3} - \frac{3}{\phi^2}\frac{d^2Q_\phi}{d\phi^2} + \frac{3}{\phi^3}\frac{dQ_\phi}{d\phi} - \frac{3}{\phi^4}Q_\phi + k^4 Q_\phi = 0$ where $k^4 = 3(1-\mu^2)\frac{a^2}{t^2}$ $Q_\phi \Big\vert_{\phi = \phi_0} = -H\phi_0$ $\quad$ $M_\phi \Big\vert_{\phi = \phi_0} = 0$
Solution	$Q_\phi = \left[\frac{C_{1H}}{k}\,\mathrm{Ber}'(k\sqrt{2}\phi) - \frac{C_{2H}}{k}\,\mathrm{Bei}'(k\sqrt{2}\phi)\right] H$
Forces	$N_\phi = (n_1 C_{1H} + n_2 C_{2H})\,H$ $N_\theta = (\eta_1 C_{1H} + \eta_2 C_{2H})\,H$ $M_\phi = (m_1 C_{1H} + m_2 C_{2H})\,Ht$ $M_\theta = \mu M_\phi + (k_1 C_{1H} + k_2 C_{2H})\,Ht$
Edge Influence Coefficients	$C_{VH} = \frac{X_a}{Et\phi_0}$ $\quad$ $C_{wH} = -\frac{W_a}{E\phi_0}$

Notes: Approximate useful range: $\phi_0 < 20°$.

For $\mathrm{Ber}'(k\sqrt{2}\phi)$, $\mathrm{Bei}'(k\sqrt{2}\phi)$ see Reference 3.

For C_{1H}, C_{2H}, W_a, and X_a as functions of $k\sqrt{2}\phi_0$ see Table B7.3.3-8.

For n_1, n_2, ... etc., as functions of $k\sqrt{2}\phi$ see Table B7.3.3-8.

TABLE B7.3.3-7 EDGE-LOADED SHALLOW SPHERICAL SHELLS (Continued)

Complete (or "Long") Spherical Shell, Shallow Opening, Constant t, Edge Moment M	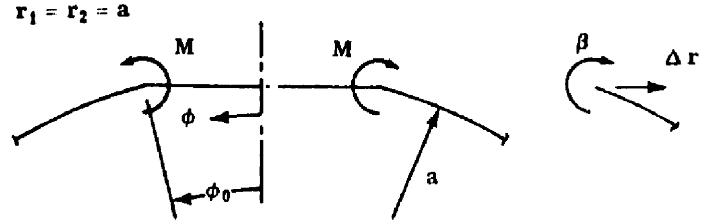
Basic	Esslinger's Approximation
Differential Equation and Boundary Conditions	$\frac{d^4Q_\phi}{d\phi^4} + \frac{2}{\phi}\frac{d^3Q_\phi}{d\phi^3} - \frac{3}{\phi^2}\frac{d^2Q_\phi}{d\phi^2} + \frac{3}{\phi^3}\frac{dQ_\phi}{d\phi} - \frac{3}{\phi^4}Q_\phi + 4k^4Q_\phi = 0$ where $k^4 = 3(1-\mu^2)\frac{a^2}{t^2}$ $Q_\phi\Big\rvert_{\phi=\phi_0} = 0 \qquad M_\phi\Big\rvert_{\phi=\phi_0} = M$
Solution	$Q_\phi = -\frac{2}{\pi}\left[\frac{C_{3M}}{k}\,\text{Kei}'(k\sqrt{2}\phi) + \frac{C_{4M}}{k}\,\text{Ker}'(k\sqrt{2}\phi)\right]\frac{M}{t}$
Forces	$N_\phi = (n_3 C_{3M} + n_4 C_{4M})\frac{M}{t}$ $N_\theta = (\eta_3 C_{3M} + \eta_4 C_{4M})\frac{M}{t}$ $M_\phi = (m_3 C_{3M} + m_4 C_{4M})M$ $M_\theta = \mu M_\phi + (k_3 C_{3M} + k_4 C_{4M})M$
Edge Influence Coefficients	$C_{VM} = \frac{X_d}{Et^2\phi_0} \qquad C_{wM} = \frac{X_c}{Et\phi_0}$

Notes: Approximate useful range: $\phi_0 < 20°$.

For $\text{Ker}'(k\sqrt{2}\phi)$, $\text{Kei}'(k\sqrt{2}\phi)$ see Reference 3.

For C_{3M}, C_{4M}, X_c, and X_d as functions of $k\sqrt{2}\phi_0$ see Table B7.3.3-8.

For n_3, n_4, ... etc. as functions of $k\sqrt{2}\phi$ see Table B7.3.3-8.

TABLE B7.3.3-7 EDGE-LOADED SHALLOW SPHERICAL SHELLS (Concluded)

Complete (or "Long") Spherical Shell, Shallow Opening, Constant t, Edge Force H	$r_1 = r_2 = a$ 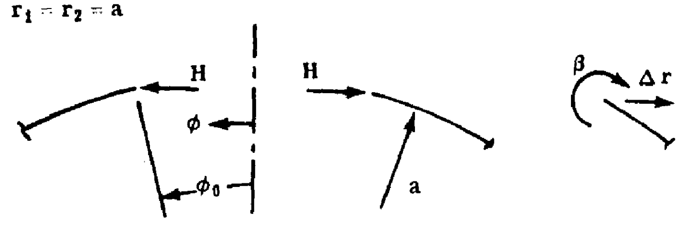
Basis	Esslinger's Approximation
Differential Equation and Boundary Conditions	$\frac{d^4Q_\phi}{d\phi^4} + \frac{2}{\phi}\frac{d^3Q_\phi}{d\phi^3} - \frac{3}{\phi^2}\frac{d^2Q_\phi}{d\phi^2} + \frac{3}{\phi^3}\frac{dQ_\phi}{d\phi} - \frac{3}{\phi^4}Q_\phi + 4k^4Q_\phi = 0$ where $k^4 = 3(1-\mu^2)\frac{a^2}{t^2}$ $Q_\phi\Big\rvert_{\phi=\phi_0} = -H\phi_0$ $\quad M_\phi\Big\rvert_{\phi=\phi_0} = 0$
Solution	$Q_\phi = -\frac{2}{\pi}\left[\frac{C_{3H}}{k}\,\mathrm{Kei}'(k\sqrt{2}\phi) + \frac{C_{4H}}{k}\,\mathrm{Ker}'(k\sqrt{2}\phi)\right]H$
Forces	$N_\phi = (n_3 C_{3H} + n_4 C_{4H})H$ $N_\theta = (\eta_3 C_{3H} + \eta_4 C_{4H})H$ $M_\phi = (m_3 C_{3H} + m_4 C_{4H})Ht$ $M_\theta = \mu M_\phi + (k_3 C_{3H} + k_4 C_{4H})Ht$
Edge Influence Coefficients	$C_{VH} = \frac{X_c}{Et\phi_0}$ $\quad C_{wH} = \frac{W_c}{E\phi_0}$

Notes: Approximate useful range: $\phi_0 < 20°$.

For $\mathrm{Ker}'(k\sqrt{2}\phi)$, $\mathrm{Kei}'(k\sqrt{2}\phi)$ see Reference 3

For C_{3H}, C_{4H}, W_c, and X_c as functions of $k\sqrt{2}\phi_0$ see Table B7.3.3-8.

For n_3, n_4, ... etc. as functions of $k\sqrt{2}\phi$ see Table B7.3.3-8.

TABLE B7.3.3-8 SHALLOW SPHERICAL SHELL COEFFICIENTS

Equations for the Esslinger Coefficients for Table B7.3.3-7

$$C_{1H} = \frac{\bar{K}_{12}}{\sqrt{2}}\left[k\sqrt{2}\phi_0\,\psi_2 - (1-\mu)\psi_1'\right]$$

$$C_{2H} = -\frac{\bar{K}_{12}}{2}\left[k\sqrt{2}\phi_0\,\psi_1 + (1-\mu)\psi_2'\right]$$

$$C_{1M} = -\bar{K}_{12}\,\psi_2'\sqrt{6(1-\mu^2)} \qquad C_{2M} = \bar{K}_{12}\,\psi_1'\sqrt{6(1-\mu^2)}$$

$$W_a = -\frac{\bar{K}_{12}}{\sqrt{12(1-\mu^2)}}\left[(k\sqrt{2}\phi_0)^3(\psi_1^2+\psi_2^2) - 2(k\sqrt{2}\phi_0)^2(\psi_1'\psi_2 - \psi_2'\psi_1) + (1-\mu^2)k\sqrt{2}\phi_0(\psi_1'^2+\psi_2'^2)\right]$$

$$X_a = -\bar{K}_{12}\left[(k\sqrt{2}\phi_0)^2(\psi_1\psi_1' + \psi_2\psi_2')\right]$$

$$X_b = -\bar{K}_{12}\sqrt{12(1-\mu^2)}\left[(k\sqrt{2}\phi_0)(\psi_1'^2+\psi_2'^2)\right]$$

$$\bar{K}_{12} = \left[\psi_1\psi_2' - \psi_2\psi_1' + \frac{1-\mu}{k\sqrt{2}\phi_0}(\psi_1'^2+\psi_2'^2)\right]^{-1}$$

$$n_1 = \sqrt{2}\,\frac{\psi_1'}{k\sqrt{2}\phi} \qquad n_2 = \sqrt{2}\,\frac{\psi_2'}{k\sqrt{2}\phi}$$

$$\eta_1 = -\sqrt{2}\left[-\psi_2 + \frac{\psi_1'}{k\sqrt{2}\phi}\right] \qquad \eta_2 = -\sqrt{2}\left[\psi_1 + \frac{\psi_2'}{k\sqrt{2}\phi}\right]$$

$$m_1 = -\frac{1}{\sqrt{6(1-\mu^2)}}\left[\psi_1 + (1-\mu)\frac{\psi_2'}{k\sqrt{2}\phi}\right]$$

$$m_2 = -\frac{1}{\sqrt{6(1-\mu^2)}}\left[\psi_2 - (1-\mu)\frac{\psi_1'}{k\sqrt{2}\phi}\right]$$

$$k_1 = \sqrt{\frac{1-\mu^2}{12}}\;n_2 \qquad k_2 = -\sqrt{\frac{1-\mu^2}{12}}\;n_1$$

ψ_1, ψ_2, ψ_1', ψ_2' are Schleicher functions and their derivatives for the argument $k\sqrt{2}\phi$ and are related to Bessel-Kelvin functions by ψ_1 = ber, ψ_2 = -bei, ψ_1' = ber', and ψ_2' = -bei'.

(Reference 1, pages 491-494, and 6-17, 6-20, and 6-32)

TABLE B7. 3. 3-8 SHALLOW SPHERICAL SHELL COEFFICIENTS (Concluded)

Equations for the Esslinger Coefficients for Table B7. 3. 3-7

$$C_{3H} = \frac{K_{34}}{\sqrt{2}} \left[k\sqrt{2}\phi_0 \, \psi_4 - (1-\mu)\psi_3' \right]$$

$$C_{4H} = -\frac{K_{34}}{\sqrt{2}} \left[k\sqrt{2}\phi_0 \, \psi_3 + (1-\mu)\psi_4' \right]$$

$$C_{3M} = -K_{34}\,\psi_4' \sqrt{6(1-\mu^2)} \qquad C_{4M} = K_{34}\,\psi_3' \sqrt{6(1-\mu^2)}$$

$$W_c = \frac{K_{34}}{\sqrt{12(1-\mu^2)}} \left[(k\sqrt{2}\phi_0)^3 (\psi_3^2 + \psi_4^2) - 2(k\sqrt{2}\phi_0)^2 (\psi_3'\psi_4 - \psi_4'\psi_3) + (1-\mu^2)\, k\sqrt{2}\phi_0 (\psi_3'^2 + \psi_4'^2) \right]$$

$$X_c = -K_{34} \left[(k\sqrt{2}\phi_0)^2 (\psi_3\psi_3' + \psi_4\psi_4') \right]$$

$$X_d = K_{34} \sqrt{12(1-\mu^2)} \left[(k\sqrt{2}\phi_0)(\psi_3'^2 + \psi_4'^2) \right]$$

$$K_{34} = \left[\psi_3\psi_4' - \psi_4\psi_3' + \frac{1-\mu}{k\sqrt{2}\phi_0} (\psi_3'^2 + \psi_4'^2) \right]^{-1}$$

$$n_3 = \sqrt{2}\,\frac{\psi_3'}{k\sqrt{2}\phi} \qquad n_4 = \sqrt{2}\,\frac{\psi_4'}{k\sqrt{2}\phi}$$

$$\eta_3 = -\sqrt{2}\left[-\psi_4 + \frac{\psi_3'}{k\sqrt{2}\phi} \right] \qquad \eta_4 = -\sqrt{2}\left[\psi_3 + \frac{\psi_4'}{k\sqrt{2}\phi} \right]$$

$$m_3 = -\frac{1}{\sqrt{6(1-\mu^2)}} \left[\psi_3 + (1-\mu)\frac{\psi_4'}{k\sqrt{2}\phi} \right]$$

$$m_4 = -\frac{1}{\sqrt{6(1-\mu^2)}} \left[\psi_4 - (1-\mu)\frac{\psi_3'}{k\sqrt{2}\phi} \right]$$

$$k_3 = \sqrt{\frac{1-\mu^2}{12}}\; n_4 \qquad k_4 = -\sqrt{\frac{1-\mu^2}{12}}\; n_3$$

ψ_3, ψ_4, ψ_3', ψ_4', are Schleicher functions and their derivatives for the argument $k\sqrt{2}\phi$ and are related to Bessel-Kelvin functions by $\psi_3 = -\frac{2}{\pi}\,\mathrm{kei}$, $\psi_4 = -\frac{2}{\pi}\,\mathrm{ker}$, $\psi_3' = -\frac{2}{\pi}\,\mathrm{kei}'$, and $\psi_4' = -\frac{2}{\pi}\,\mathrm{ker}'$.

(Reference 1, pages 491-494, and 6-17, 6-20, and 6-32)

B7.3.3.4 Cylindrical Shells

This paragraph presents the solutions for long and short cylinders, loaded along the boundary with the unit-edge loadings (moments, shear, forced horizontal displacement, and forced rotation at the boundary). All disturbances in the cylindrical wall caused by edge loading will become, for practical purposes, negligible at distance $x = \sqrt{Rt}$. If the height of the cylinder is less than x, the analyst is dealing with a circular ring instead of a shell. Further, to be conservative, the following precautions should be taken.

a. If $kL \leq 5$, the more exact theory is used, and such cylinders are designated as short cylinders.

b. If $kL \geq 5$, the simplified formula is used; this is a special case of the more general case a.

The constant k is defined as follows:

$$k^4 = 3(1 - \mu^2)/R^2 t^2 \quad .$$

The primary solutions (membrane theory) will not be affected by the length of the cylinder. The boundaries must be free to rotate and deflect because of the action of the unit-edge loadings. The shell thickness must be uniform in the range where the stresses are present.

I Long Cylinders

The formulas for the disturbances caused by unit-edge loadings are presented in Table B7.3.3-9. In this table,

$$D = \frac{Et^3}{12(1 - \mu^2)} \quad .$$

TABLE B7.3.3-9 LONG CYLINDRICAL SHELLS, UNIT-EDGE LOADING SOLUTIONS

	Q = 1	M = 1
	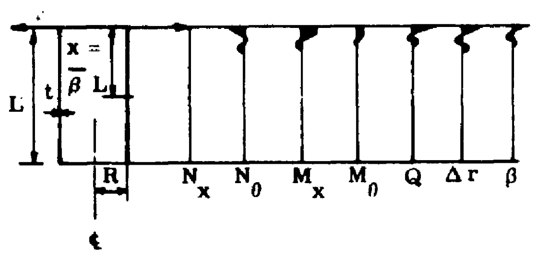	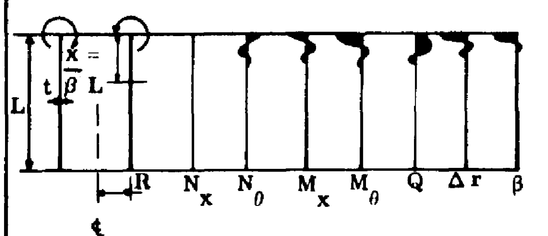
N_x	0	0
N_θ	$-\frac{2Rk}{L} e^{-k\bar{\beta}} \cos k\bar{\beta}$	$\frac{2\sqrt{2} \cdot Rk^2}{L^2} e^{-k\bar{\beta}} \cos\left(k\bar{\beta} + \frac{\pi}{4}\right)$
M_x	$\frac{L}{k} e^{-k\bar{\beta}} \sin k\bar{\beta}$	$-\sqrt{2} \cdot e^{-k\bar{\beta}} \sin\left(k\bar{\beta} + \frac{\pi}{4}\right)$
M_θ	μM_x	μM_x
Q	$\sqrt{2} \cdot e^{-k\bar{\beta}} \cos\left(k\bar{\beta} + \frac{\pi}{4}\right)$	$\frac{2k}{L} e^{-k\bar{\beta}} \sin k\bar{\beta}$
β	$\frac{L^2}{\sqrt{2} \cdot k^2 D} e^{-k\bar{\beta}} \sin\left(k\bar{\beta} + \frac{\pi}{4}\right)$	$-\frac{L}{Dk} e^{-k\bar{\beta}} \cos k\bar{\beta}$
Δr	$-\frac{R}{Et}\left(N_\theta - \mu N_x\right) = \frac{L^3}{2Dk^3} e^{-k\bar{\beta}} \cos k\bar{\beta}$	$-\frac{R}{Et}\left(N_\theta - \mu N_x\right) = -\frac{L^3}{\sqrt{2}Dk^2} e^{-k\bar{\beta}} \cos\left(k\bar{\beta} + \frac{\pi}{4}\right)$

For the Case $\bar{\beta} = 0$

β	$\frac{L^2}{2k^2D}$	$\frac{-L}{Dk}$
Δr	$\frac{L^3}{2k^3D}$	$\frac{-L^2}{2Dk^2}$

II Short Cylinders

The following constants are used for Tables B7.3.3-10 and B7.3.3-11:

$$k^4 = 3(1-\mu^2)/R^2 t^2$$

$$\rho = \sinh^2 \beta L - \sin^2 \beta L$$

$$K_1 = (\sinh \beta L \cosh \beta L - \sin \beta L \cos \beta L)/\rho$$

$$K_2 = (\sin \beta L \cosh \beta L - \cos \beta L \sinh \beta L)/\rho$$

$$K_3 = (\sinh^2 \beta L + \sin^2 \beta L)/\rho$$

$$K_4 = 2 \sinh \beta L \sin \beta L/\rho$$

$$K_5 = 2(\sin \beta L \cos \beta L + \sinh \beta L \cosh \beta L)/\rho$$

$$K_6 \quad 2(\sin \beta L \cosh \beta L + \cos \beta L \sinh \beta L)/\rho$$

The formulas for unit-edge loading disturbances are presented in Tables B7.3.3-10 and B7.3.3-11. To use these formulas the relation $\beta L \leq 5$ must be satisfied.

A summary of edge distortions resulting from edge loadings is given in Table B7.3.3-12.

B7.3.3.5 Conical Shells

This paragraph presents the solutions for nonshallow open or closed conical shells in which α_0 is not small. There is no exact information about limiting angle α_0. It is recommended that consideration be limited to the range of $\alpha_0 \geq 45°$. If $\alpha_0 = 90°$, the cone degenerates into a cylinder.

TABLE B7.3.3-10 CYLINDRICAL SHELLS, EXACT FORMULAS FOR UNIT-EDGE LOADING SOLUTIONS

	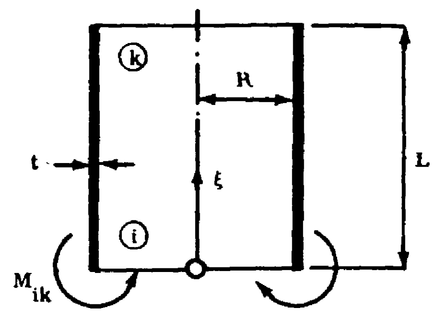	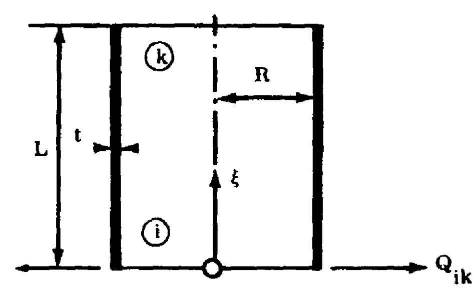
N_θ	$M_{ik}\, 2k^2R\left[-\frac{F_2}{F_1}F_7(\xi) + \frac{F_3}{F_1}F_{10}(\xi) - F_8(\xi)\right]$	$Q_{ik}\, 2kR\left[\frac{F_4}{F_1}F_7(\xi) - \frac{F_5}{F_1}F_{15}(\xi) - \frac{F_6}{F_1}F_{16}(\xi)\right]$
M_x	$M_{ik}\left[\frac{F_2}{F_1}F_8(\xi) - \frac{F_3}{F_1}F_9(\xi) - F_7(\xi)\right]$	$\frac{Q_{ik}}{k}\left[-\frac{F_4}{F_1}F_8(\xi) - \frac{F_5}{F_1}F_{16}(\xi) + \frac{F_6}{F_1}F_{15}(\xi)\right]$
Q_x	$-kM_{ik}\left[\frac{F_2}{F_1}F_{10}(\xi) - \frac{2F_3}{F_1}F_8(\xi) + F_8(\xi)\right]$	$Q_{ik}\left[\frac{F_4}{F_1}F_{10}(\xi) + \frac{F_5}{F_1}F_{13}(\xi) - \frac{F_6}{F_1}F_{14}(\xi)\right]$
Δr	$\frac{M_{ik}}{2Dk^2}\left[-\frac{F_2}{F_1}F_7(\xi) + \frac{F_3}{F_1}F_{10}(\xi) - F_8(\xi)\right]$	$\frac{Q_{ik}}{2Dk^3}\left[\frac{F_4}{F_1}F_7(\xi) - \frac{F_5}{F_1}F_{15}(\xi) - \frac{F_6}{F_1}F_{16}(\xi)\right]$
β	$\frac{M_{ik}}{2Dk}\left[\frac{F_2}{F_1}F_9(\xi) + \frac{2F_3}{F_1}F_7(\xi) - F_{10}(\xi)\right]$	$-\frac{Q_{ik}}{2Dk^2}\left[\frac{F_4}{F_1}F_9(\xi) + \frac{F_5}{F_1}F_{14}(\xi) + \frac{F_6}{F_1}F_{13}(\xi)\right]$

TABLE B7.3.3-11 CYLINDRICAL SHELLS, EXACT FORMULAS FOR UNIT-EDGE DEFORMATIONS

	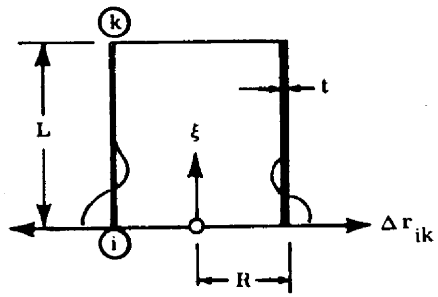	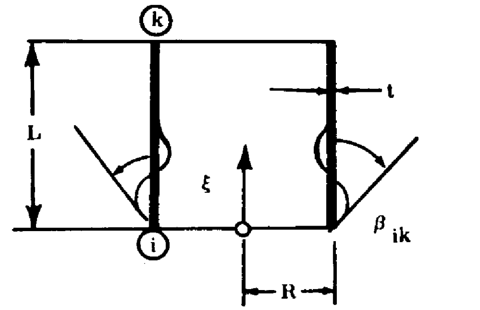
N_θ	$\Delta r_{ik} \frac{Et}{R} \left[F_7(\xi) + \frac{F_3}{F_1} F_9(\xi) - \frac{F_2}{F_1} F_8(\xi) \right]$	$\frac{\beta_{ik}}{k} \frac{Et}{R} \left[\frac{F_6}{F_1} F_{15}(\xi) - \frac{F_5}{F_1} F_{16}(\xi) - \frac{F_4}{F_1} F_8(\xi) \right]$
M_x	$\Delta r_{ik}\, 2Dk^2 \left[-F_8(\xi) + \frac{F_3}{F_1} F_{10}(\xi) - \frac{F_2}{F_1} F_7(\xi) \right]$	$\beta_{ik}\, 2Dk \left[\frac{F_6}{F_1} F_{16}(\xi) + \frac{F_5}{F_1} F_{15}(\xi) - \frac{F_4}{F_1} F_7(\xi) \right]$
Q_x	$\Delta r_{ik}\, 2Dk^3 \left[-F_{10}(\xi) + 2\frac{F_3}{F_1} F_7(\xi) + \frac{F_2}{F_1} F_9(\xi) \right]$	$-\beta_{ik}\, 2Dk^2 \left[\frac{F_6}{F_1} F_{13}(\xi) + \frac{F_5}{F_1} F_{14}(\xi) + \frac{F_4}{F_1} F_9(\xi) \right]$
Δr	$\Delta r_{ik}\, k \left[F_7(\xi) + \frac{F_3}{F_1} F_9(\xi) - \frac{F_2}{F_1} F_8(\xi) \right]$	$\frac{\beta_{ik}}{k} \left[\frac{F_6}{F_1} F_{15}(\xi) - \frac{F_5}{F_1} F_{16}(\xi) - \frac{F_4}{F_1} F_8(\xi) \right]$
β	$\Delta r_{ik}\, k \left[-F_9(\xi) + 2\frac{F_3}{F_1} F_8(\xi) - \frac{F_2}{F_1} F_{10}(\xi) \right]$	$\beta_{ik} \left[\frac{F_6}{F_1} F_{14}(\xi) - \frac{F_5}{F_1} F_{13}(\xi) - \frac{F_4}{F_1} F_{10}(\xi) \right]$

TABLE B7.3.3-12 CYLINDRICAL SHELLS EDGE DISTORTIONS RESULTING FROM EDGE LOADINGS

Loading Condition \ Edge Distortions	ΔH_{ik}	β_{ik}	ΔH_{ki}	β_{ki}
Q_{ik}	$-Q_{ik}\frac{2R^2k}{Et}\frac{F_4}{F_1}$	$Q_{ik}\frac{2R^2k^2}{Et}\frac{F_2}{F_1}$	$Q_{ki}\frac{2R^2k}{Et}\frac{F_9}{F_1}$	$Q_{ik}\frac{2R^2k^2}{Et}\frac{2F_8}{F_1}$
M_{ik}	$M_{ik}\frac{2R^2k^2}{Et}\frac{F_2}{F_1}$	$-M_{ik}\frac{2R^2k^3}{Et}\frac{2F_3}{F_1}$	$-M_{ik}\frac{2R^2k^2}{Et}\frac{2F_8}{F_1}$	$-M_{ik}\frac{2R^2k^3}{Et}\frac{2F_{10}}{F_1}$
Q_{ki}	$-Q_{ki}\frac{2R^2k}{Et}\frac{F_9}{F_1}$	$Q_{ki}\frac{2R^2k^2}{Et}\frac{2F_3}{F_1}$	$Q_{ki}\frac{2R^2k}{Et}\frac{F_4}{F_1}$	$Q_{ki}\frac{2R^2k^2}{Et}\frac{F_2}{F_1}$
M_{ki}	$-M_{ki}\frac{2R^2k^2}{Et}\frac{2F_8}{F_1}$	$M_{ki}\frac{2R^2k^3}{Et}\frac{2F_{10}}{F_1}$	$M_{ki}\frac{2R^2k^2}{Et}\frac{F_2}{F_1}$	$M_{ki}\frac{2R^2k^3}{Et}\frac{2F_3}{F_1}$

Another limitation must be applied to the height of the cone. As in the case of the sphere, the disturbances due to unit-edge loadings will decay at a short distance from the disturbed edge (for practical purposes, approximately at $\sqrt{R_0 t}$). Consequently, a "high" cone is characterized by an undisturbed edge (or apex) as a result of unit-loading influences on the respective opposite edge.

The boundaries must be free to rotate and deflect vertically and horizontally as a result of the action of the unit-edge loadings. Abrupt discontinuities in the shell thickness must not be present. The thickness of the shell must be uniform in the range in which the stresses exist.

The formulas are assembled for closed and open conical shells. Open conical shells are characterized by removal of the upper part above some circumference in the plane parallel to the base.

Linear bending theory was used to derive the following formulas. If the height of the segment is less than $\sqrt{Rt}$, the analyst is practically dealing with a circular ring instead of a shell. The following constants are important:

$$k = \frac{h}{\sqrt{R_0 t \sin\phi}} \quad \sqrt[4]{3(1-\mu^2)} \quad , \quad R_0 = \text{MAX } R$$

$$D = \frac{Et^3}{12(1-\mu^2)} \quad .$$

Additional designations are indicated in Figure B7.3.3-4.

R is variable and is perpendicular to the meridian. Angle (ϕ) is constant. Table B7.3.3-13 presents the formulas for a closed conical shell.

I Open Conical Shell, Unit Loading at Lower Edge

Since unit influences are not progressing very far from the edge into the cone, the formulas presented in Table B7.3.3-13 can be used for the cone with opening at vertex (Figure B7.3.3-5).

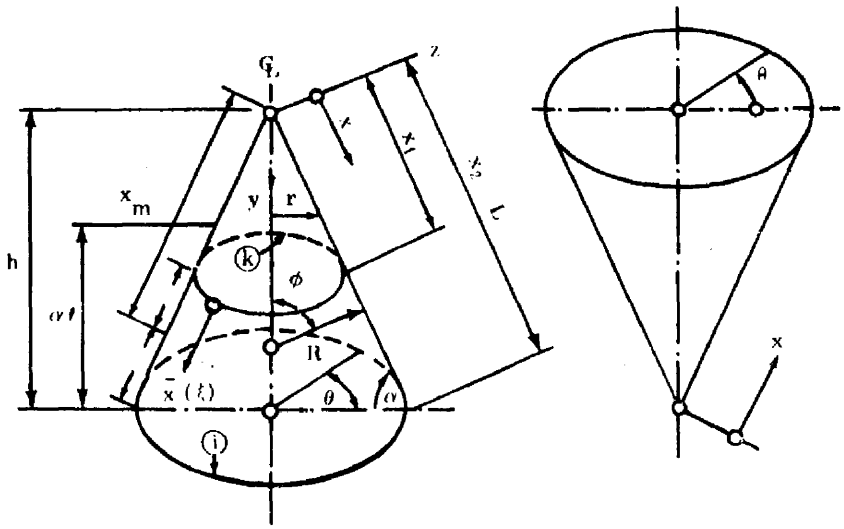

FIGURE B7.3.3-4 CONE NOMENCLATURE

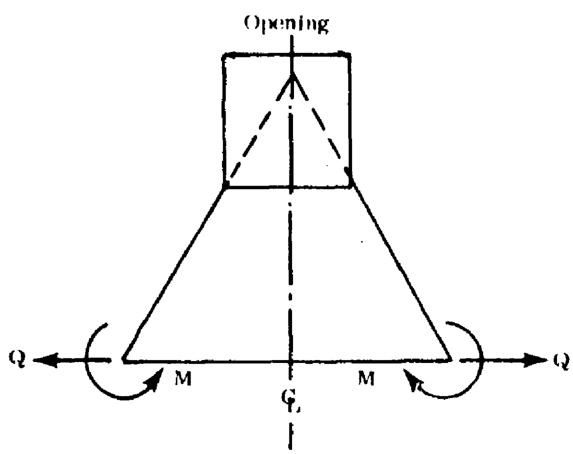

FIGURE B7.3.3-5 OPEN CONICAL SHELL LOADING
AT LOWER EDGE

TABLE B7. 3. 3-13 CONICAL SHELL, UNIT-EDGE LOADING SOLUTIONS

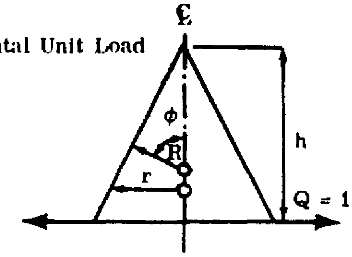

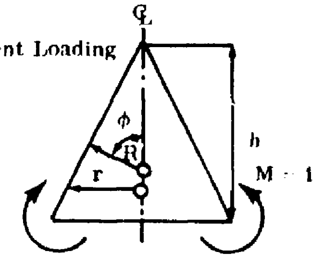

N_ϕ	$-\sqrt{2}\cos\phi \cdot e^{-k\alpha}\cos\left(k\alpha + \frac{\pi}{4}\right)$	$-\frac{2k\cos\phi}{h} e^{-k\alpha}\sin k\alpha$
N_θ	$-\frac{2R^2 k\sin^2\phi}{h} e^{-k\alpha}\cos k\alpha$	$\frac{2\sqrt{2}Rk^2\sin^2\phi}{h^2} e^{-k\alpha}\cos\left(k\alpha + \frac{\pi}{4}\right)$
M_ϕ	$\frac{h}{k} e^{-k\alpha}\sin k\alpha$	$-\sqrt{2}\, e^{-k\alpha}\sin\left(k\alpha + \frac{\pi}{4}\right)$
M_θ	$\frac{h^2}{\sqrt{2}Rk^2}\frac{\cot\phi}{\sin\phi} e^{-k\alpha}\sin\left(k\alpha + \frac{\pi}{4}\right) + \mu M_\phi$	$-\frac{h\cot\phi\, e^{-k\alpha}\cos k\alpha}{Rk\sin\alpha} + \mu M_\phi$
Q	$-\sqrt{2}\sin\phi \cdot e^{-k\alpha}\cos\left(k\alpha + \frac{\pi}{4}\right)$	$-\frac{2k\sin\phi}{h} e^{-k\alpha}\sin k\alpha$
Deformations		
Δr	$\frac{h^3 e^{-k\alpha}}{2Dk^3\sin\phi}\left[\cos k\alpha - \frac{h}{\sqrt{2}Rk}\frac{\cos\phi}{\sin\phi}\cos\left(k\alpha + \frac{\pi}{4}\right)\right]$	$\frac{-h^2 e^{-k\alpha}}{2Dk^2\sin\phi}\left[\sqrt{2}\cos\left(k\alpha + \frac{\pi}{4}\right) + \mu\frac{h}{R}\frac{\cos\phi\sin k\alpha}{k\sin^2\phi}\right]$
β	$-\frac{h^2 e^{-k\alpha}\sin\left(k\alpha + \frac{\pi}{4}\right)}{\sqrt{2}Dk^2\sin\phi}$	$\frac{h e^{-k\alpha}\cos k\alpha}{Dk\sin\phi}$
For $\alpha = 0$		
Δr	$\frac{h^3}{2Dk^3\sin\phi}\left[1 - \frac{\mu h\cot\phi}{2Rk\sin\phi}\right]$	$-\frac{h^2}{2Dk^2\sin\phi}$
β	$-\frac{n^2}{2Dk^2\sin\phi}$	$\frac{h}{Dk\sin\phi}$

II Open Conical Shell, Unit Loading at Upper Edge

If it is imagined that the shell, loaded as shown in Figure B7.3.3-6(A), is replaced with shell as shown in Figure B7.3.3-6(B), the result is a conical shell loaded with unit loading at the lower edge. The same formulas are used for determining edge influence, but it is noted that $\phi > 90°$.

An additional set of formulas for open conical shells (that can be also used for closed cone) is presented in Table B7.3.3-14. These formulas are expressed with the functions F_i and $F_i(\xi)$, which are tabulated in Paragraph B7.3.3.2. The following constant is used for k:

$$k = \frac{\sqrt[4]{3(1-\mu^2)}}{\sqrt{t x_m \cot \alpha_0}} .$$

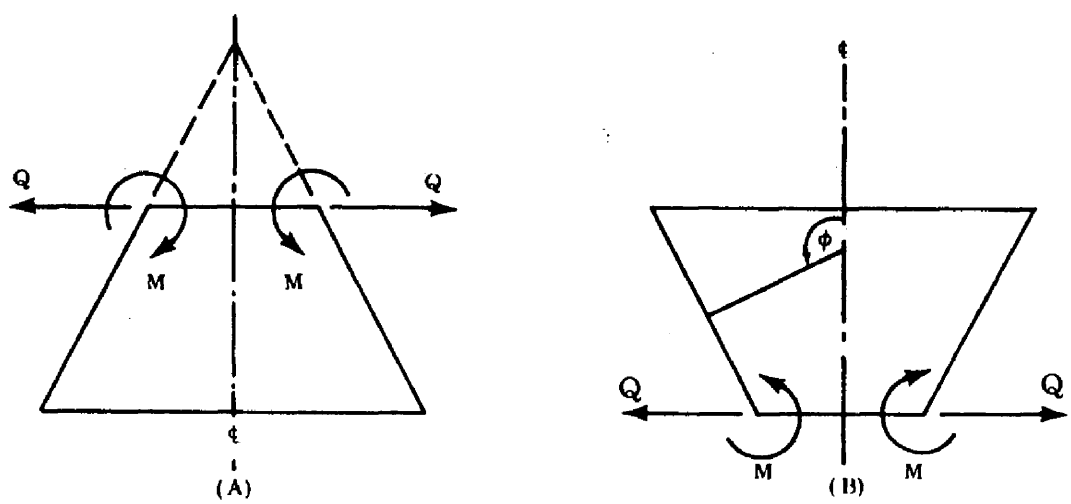

FIGURE B7.3.3-6 OPEN CONICAL SHELL LOADING AT UPPER EDGE

TABLE B7.3.3-14 OPEN CONICAL SHELL, UNIT-EDGE LOADING SOLUTIONS

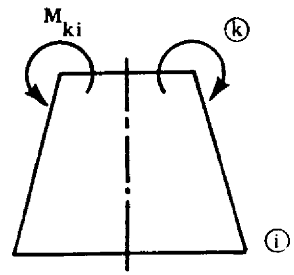

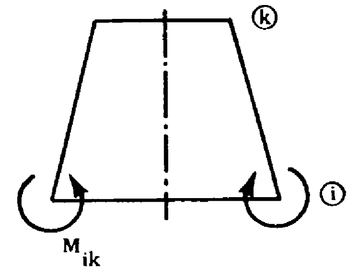

N_x	$M_{ki}\, 2k \cot\alpha_0 \left[\frac{F_6}{F_1} F_{15}(\xi) + \frac{F_5}{F_1} F_{16}(\xi) - \frac{F_3}{F_1} F_8(\xi)\right]$	$M_{ik}\, 2k \cot\alpha_0 \left[\frac{F_8}{F_2} F_{10}(\xi) - \frac{F_{10}}{F_1} F_8(\xi)\right]$
N_θ	$M_{ki}\, 2k^2 x_m \cot\alpha_0 \left[\frac{F_6}{F_1} F_{14}(\xi) + \frac{F_5}{F_1} F_{13}(\xi) - \frac{F_3}{F_1} F_{10}(\xi)\right]$	$M_{ik}\, 2k^2 x_m \cot\alpha_0 \left[\frac{2F_8}{F_1} F_7(\xi) - \frac{F_{10}}{F_1} F_{10}(\xi)\right]$
M_x	$M_{ki} \left[\frac{F_6}{F_1} F_{13}(\xi) - \frac{F_5}{F_1} F_{14}(\xi) + \frac{F_3}{F_1} F_9(\xi)\right]$	$-M_{ik} \left[\frac{2F_8}{F_1} F_8(\xi) - \frac{F_{10}}{F_1} F_9(\xi)\right]$
Q_x	$M_{ki}\, 2k \left[\frac{F_6}{F_1} F_{15}(\xi) + \frac{F_5}{F_1} F_{16}(\xi) - \frac{F_3}{F_1} F_8(\xi)\right]$	$M_{ik}\, 2k \left[\frac{F_8}{F_1} F_{10}(\xi) - \frac{F_{10}}{F_1} F_8(\xi)\right]$
Δr	$M_{ki} \frac{\sin\alpha_0}{2Dk^2} \left[\frac{F_6}{F_1} F_{14}(\xi) + \frac{F_5}{F_1} F_{13}(\xi) - \frac{F_3}{F_1} F_{10}(\xi)\right]$	$M_{ik} \frac{\sin\alpha_0}{2Dk^2} \left[\frac{2F_8}{F_1} F_7(\xi) - \frac{F_{10}}{F_1} F_{10}(\xi)\right]$
β	$-\frac{M_{ik}}{Dk} \left[\frac{F_6}{F_1} F_{16}(\xi) - \frac{F_5}{F_1} F_{15}(\xi) - \frac{F_3}{F_1} F_7(\xi)\right]$	$M_{ik} \frac{1}{Dk} \left[\frac{F_8}{F_1} F_9(\xi) + \frac{F_{10}}{F_1} F_7(\xi)\right]$

TABLE B7. 3. 3-14 OPEN CONICAL SHELL, UNIT-EDGE LOADING SOLUTIONS (Concluded)

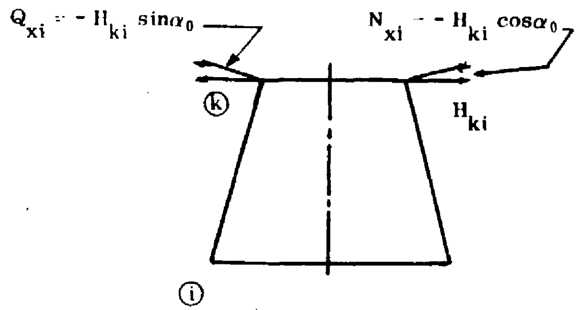

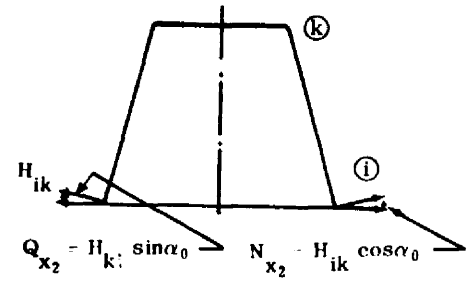

N_x	$-H_{ki}\cos\alpha_0\left[F_7(\xi) - \frac{F_4}{F_1}F_{10}(\xi) + \frac{F_2}{F_1}F_8(\xi)\right]$	$H_{ki}\cos\alpha_0\left[-\frac{F_9}{F_1}F_{10}(\xi) + \frac{2F_8}{F_1}F_8(\xi)\right]$
N_θ	$H_{ki}\,x_m\,k\cos\alpha_0\left[F_9(\xi) + \frac{2F_4}{F_1}F_7(\xi) - \frac{F_2}{F_1}F_{10}(\xi)\right]$	$2H_{ik}\,x_m\cos\alpha_0\left[-\frac{F_9}{F_1}F_7(\xi) + \frac{F_8}{F_1}F_{10}(\xi)\right]$
M_x	$H_{ki}\frac{\sin\alpha_0}{2}\left[F_{10}(\xi) - \frac{2F_4}{F_1}F_8(\xi) + \frac{F_2}{F_1}F_9(\xi)\right]$	$H_{ik}\frac{\sin\alpha_0}{k}\left[\frac{F_9}{F_1}F_8(\xi) - \frac{F_8}{F_1}F_9(\xi)\right]$
Q_x	$-H_{ki}\sin\alpha_0\left[F_7(\xi) - \frac{F_4}{F_1}F_{10}(\xi) + \frac{F_2}{F_1}F_8(\xi)\right]$	$H_{ik}\sin\alpha_0\left[-\frac{F_9}{F_1}F_{10}(\xi) + \frac{2F_8}{F_1}F_8(\xi)\right]$
Δr	$H_{ki}\frac{\sin^2\alpha_0}{4Dk^3}\left[F_9(\xi) + \frac{2F_4}{F_1}F_7(\xi) - \frac{F_2}{F_1}F_{10}(\xi)\right]$	$H_{ik}\frac{\sin^2\alpha_0}{2Dk^3}\left[-\frac{F_9}{F_1}F_7(\xi) + \frac{F_8}{F_1}F_{10}(\xi)\right]$
β	$H_{ki}\frac{\sin\alpha_0}{2Dk^2}\left[-F_8(\xi) + \frac{F_4}{F_1}F_9(\xi) + \frac{F_2}{F_1}F_7(\xi)\right]$	$-H_{ik}\frac{\sin\alpha_0}{2Dk^2}\left[+\frac{F_9}{F_1}F_9(\xi) + \frac{2F_8}{F_1}F_7(\xi)\right]$

In connection with some problems, it may be of interest to know the stresses and displacements in the conical shell (closed or open), if unit displacements at the edges are acting instead of M and Q:

At lower boundary i:
- Δr_{ik} = unit displacement in horizontal direction
- β_{ik} = unit rotation.

At upper boundary k:
- Δr_{ik} = unit displacement in horizontal direction
- β_{ik} = unit rotation.

Table B7.3.3-15(a) supplies the answer to this problem. Table B7.3.3-15(b) presents a summary of edge distortions resulting from secondary loading of a conical segment with free edges.

B7.3.3.6 Circular Plates

A collection of solutions for circular plates with different axisymmetrical loading conditions is presented in this section. Circular plates with and without a central circular hole are considered. These solutions can be used individually or in the process of interaction with more complicated structures. The following nomenclature will be used:

w = deflection

β = rotation

E = Young's modulus

μ = Poisson's ratio

t = thickness of plate

$$D = \frac{Et^3}{12(1-\mu^2)}$$

TABLE B7. 3. 3-15(a) OPEN CONICAL SHELL, UNIT-EDGE LOADING SOLUTIONS

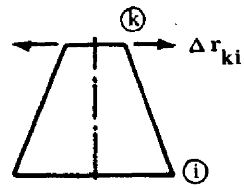

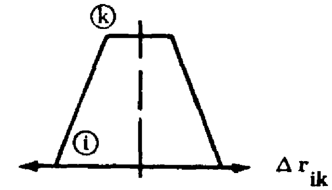

N_x	$\dfrac{4Dk^3 \cot \alpha_0 \, \Delta r_{ki}}{\sin \alpha_0} \left[- \dfrac{F_3}{F_1} F_7(\xi) - \dfrac{F_5}{F_1} F_{15}(\xi) + \dfrac{F_6}{F_1} F_{16}(\xi) \right]$	$\dfrac{4Dk^3 \cot \alpha_0 \, \Delta r_{ik}}{\sin \alpha_0} \left[\dfrac{F_{10}}{F_1} F_7(\xi) + \dfrac{F_8}{F_1} F_9(\xi) \right]$
N_θ	$\dfrac{Et \, \Delta r_{ki}}{x_m \cos \alpha_0} \left[\dfrac{F_3}{F_1} F_9(\xi) - \dfrac{F_5}{F_1} F_{14}(\xi) + \dfrac{F_6}{F_1} F_{13}(\xi) \right]$	$\dfrac{Et \, \Delta r_{ik}}{x_m \cos \alpha_0} \left[- \dfrac{F_{10}}{F_1} F_9(\xi) + \dfrac{2F_8}{F_1} F_8(\xi) \right]$
M_x	$\dfrac{2Dk^2 \, \Delta r_{ki}}{\sin \alpha_0} \left[\dfrac{F_3}{F_1} F_{10}(\xi) - \dfrac{F_5}{F_1} F_{13}(\xi) - \dfrac{F_6}{F_1} F_{14}(\xi) \right]$ $M_\phi = \mu M_x$	$\dfrac{2Dk^2 \, \Delta r_{ik}}{\sin \alpha_0} \left[- \dfrac{F_{10}}{F_1} F_{10}(\xi) + \dfrac{2F_8}{F_1} F_7(\xi) \right]$
Q_x	$\dfrac{4Dk^3 \, \Delta r_{ki}}{\sin \alpha_0} \left[- \dfrac{F_3}{F_1} F_7(\xi) - \dfrac{F_5}{F_1} F_{15}(\xi) + \dfrac{F_6}{F_1} F_{16}(\xi) \right]$	$\dfrac{4Dk^3 \, \Delta r_{ik}}{\sin \alpha_0} \left[\dfrac{F_{10}}{F_1} F_9(\xi) + \dfrac{F_8}{F_1} F_9(\xi) \right]$
Δr	$\Delta r = \Delta r_{ki} \left[\dfrac{F_3}{F_1} F_9(\xi) - \dfrac{F_5}{F_1} F_{14}(\xi) + \dfrac{F_6}{F_1} F_{13}(\xi) \right]$	$\Delta r_{ik} \left[- \dfrac{F_{10}}{F_1} F_9(\xi) + \dfrac{2F_8}{F_1} F_8(\xi) \right]$
β	$- \dfrac{2k}{\sin \alpha_0} \Delta r_{ki} \left[\dfrac{F_3}{F_1} F_8(\xi) - \dfrac{F_5}{F_1} F_{16}(\xi) - \dfrac{F_6}{F_1} F_{15}(\xi) \right]$	$\dfrac{2k \, \Delta r_{ik}}{\sin \alpha_0} \left[\dfrac{F_{10}}{F_1} F_8(\xi) - \dfrac{F_8}{F_1} F_{16}(\xi) - \dfrac{F_8}{F_1} F_{15}(\xi) \right]$

TABLE B7.3.3-15(a) OPEN CONICAL SHELL, UNIT-EDGE LOADING SOLUTIONS (Concluded)

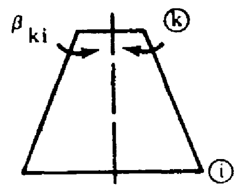

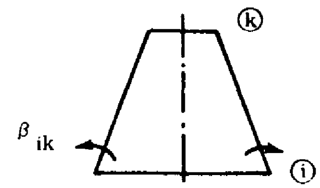

N_x	$2Dk^2 \cot \alpha_0 \beta_{ki} \left[\frac{F_2}{F_1} F_7(\xi) + \frac{F_4}{F_1} F_9(\xi) - F_8(\xi)\right]$	$2Dk^2 \cot \alpha_0 \beta_{ik} \left[\frac{2F_8}{F_1} F_7(\xi) + \frac{F_9}{F_1} F_9(\xi)\right]$
N_θ	$2Dk^3 x_m \cot \alpha_0 \beta_{ki} \left[- \frac{F_2}{F_1} F_9(\xi) + \frac{2F_4}{F_1} F_8(\xi) - F_{10}(\xi)\right]$	$4Dk^3 x_m \cot \alpha_0 \beta_{ik} \left[- \frac{F_8}{F_1} F_9(\xi) + \frac{F_9}{F_1} F_8(\xi)\right]$
M_x	$Dk \beta_{ki} \left[- \frac{F_2}{F_1} F_{10}(\xi) + \frac{2F_4}{F_1} F_7(\xi) + F_9(\xi)\right]$	$2Dk \beta_{ik} \left[- \frac{F_8}{F_1} F_{10}(\xi) + \frac{F_9}{F_1} F_7(\xi)\right]$
Q_x	$2Dk^2 \beta_{ki} \left[\frac{F_2}{F_1} F_7(\xi) + \frac{F_4}{F_1} F_9(\xi) - F_8(\xi)\right]$	$2Dk^2 \beta_{ik} \left[\frac{2F_8}{F_1} F_7(\xi) + \frac{F_9}{F_1} F_9(\xi)\right]$
Δr	$\frac{\sin \alpha_0}{2k} \beta_{ki} \left[- \frac{F_2}{F_1} F_9(\xi) + \frac{2F_4}{F_1} F_8(\xi) - F_{10}(\xi)\right]$	$\frac{\sin \alpha_0}{k} \beta_{ik} \left[- \frac{F_8}{F_1} F_9(\xi) + \frac{F_9}{F_1} F_8(\xi)\right]$
β	$\beta_{ki} \left[\frac{F_2}{F_1} F_8(\xi) - \frac{F_4}{F_1} F_{10}(\xi) + F_7(\xi)\right]$	$\beta_{ik} \left[\frac{2F_8}{F_1} F_8(\xi) - \frac{F_9}{F_1} F_{10}(\xi)\right]$

TABLE B7. 3. 3-15(b) CONICAL SEGMENT WITH FREE EDGES. EDGE DISTORTIONS RESULTING FROM SECONDARY LOADINGS

Edge Distortion / Loading Condition	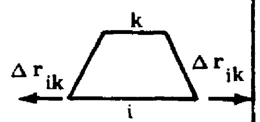	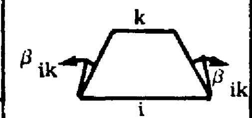	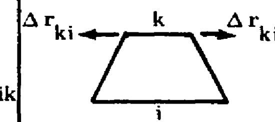	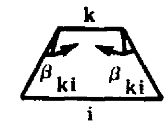
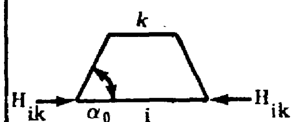	$-H_{ik}\frac{\sin^2\alpha_0}{2Dk^3}\frac{F_4}{F_1}$	$+H_{ik}\frac{\sin\alpha_0}{2Dk^2}\frac{F_2}{F_1}$	$+H_{ik}\frac{\sin^2\alpha_0}{2Dk^3}\frac{F_8}{F_1}$	$+H_{ik}\frac{\sin\alpha_0}{2Dk^2}\frac{2F_8}{F_1}$
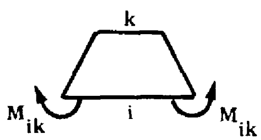	$+M_{ik}\frac{\sin\alpha_0}{2Dk^2}\frac{F_2}{F_1}$	$-M_{ik}\frac{1}{2Dk}\frac{2F_3}{F_1}$	$-M_{ik}\frac{\sin\alpha_0}{2Dk^2}\frac{2F_8}{F_1}$	$-M_{ik}\frac{1}{2Dk}\frac{2F_{10}}{F_1}$
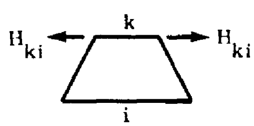	$-H_{ki}\frac{\sin^2\alpha_0}{2Dk^3}\frac{F_9}{F_1}$	$+H_{ki}\frac{\sin\alpha_0}{2Dk^2}\frac{2F_8}{F_1}$	$+H_{ki}\frac{\sin^2\alpha_0}{2Dk^3}\frac{F_4}{F_1}$	$+H_{ki}\frac{\sin\alpha_0}{2Dk^2}\frac{F_2}{F_1}$
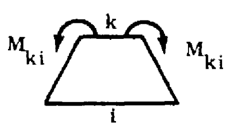	$-M_{ki}\frac{\sin\alpha_0}{2Dk^2}\frac{2F_8}{F_1}$	$+M_{ki}\frac{1}{2Dk}\frac{2F_{10}}{F_1}$	$+M_{ki}\frac{\sin\alpha_0}{2Dk^2}\frac{F_2}{F_1}$	$+M_{ki}\frac{1}{2Dk}\frac{2F_3}{F_1}$

M_r = radial moment

M_t = tangential moment

Q_r = radial shear.

Other designations are indicated in tables presented in this section.

The formulas presented were derived by using the linear bending theory. The "primary" solution is presented first; then "secondary" solutions are presented in the same way as for the shells. Finally, special cases (fixed boundary conditions) will be given.

I Primary Solutions

Primary solutions are assembled in Tables B7.3.3-16 and B7.3.3-17.

II Secondary Solutions

The only unit-edge loading of importance is a unit moment loading along the edges (Figure B7.3.3-7). Table B7.3.3-18 presents solutions for this loading for different cases of circular plate with and without the circular opening at the center. Table B7.3.3-19 presents the stresses in circular plates resulting from edge elongation.

III Special Cases

Special cases and solutions for circular plates that occur commonly in practice are presented in this paragraph. The geometry, boundary conditions, and loadings for special circular plates (with and without a central hole) are shown in Tables B7.3.3-20, B7.3.3-21, and B7.3.3-22.

TABLE B7. 3. 3-16 SIMPLY SUPPORTED CIRCULAR PLATES

Loading Constant

$p = \text{const.}\,;\ P = pa^2 w$

$A = \dfrac{P}{2aw}\ ;\ Q_r = \dfrac{P\rho}{2aw}$

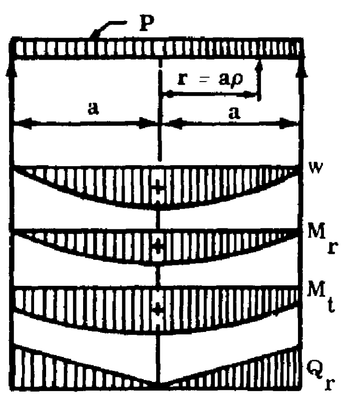

Parabolic Distribution

$p = p_o(1 - \rho^2)\,;\ P = p_o a^2 \dfrac{w}{2}$

$A = \dfrac{P}{2aw}\ ;\ Q_r = \dfrac{P\rho(2 - \rho^2)}{2wa}$

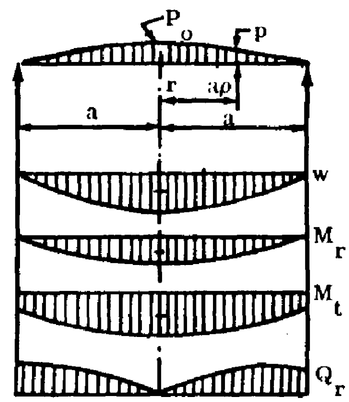

w	$\dfrac{Pa^2(1-\rho)}{64D\pi}\left(\dfrac{5+\mu}{1+\mu} - \rho^2\right)$	$\dfrac{Pa^2}{288D\pi}\left(\dfrac{31+7\mu}{1+\mu} - \dfrac{39+15\mu}{1+\mu} - \rho^2 + 9\rho^4 - \rho^6\right)$
β	$\dfrac{Pa\rho}{16D\pi}\left(\dfrac{3+\mu}{1+\mu} - \rho^2\right)$	$\dfrac{Pa\rho}{48D\pi}\left(\dfrac{13+5\mu}{1+\mu} - 6\rho^2 + \rho^4\right)$
M_r	$\dfrac{P}{16\pi}(3+\mu)(1-\rho^2)$	$\dfrac{P}{48\pi}\left[13 + 5\mu - 6(3+\mu)\rho^2 + (5+\mu)\rho^4\right]$
M_t	$\dfrac{P}{16\pi}\left[3 + \mu - (1+3\mu)\rho^2\right]$	$\dfrac{P}{48\pi}\left[13 + 5\mu - 6(1+3\mu)\rho^2 + (1+5\mu)\rho^4\right]$

TABLE B7.3.3-16 SIMPLY SUPPORTED CIRCULAR PLATES (Continued)

Conical Distribution

$p = p_o(1-\rho)\ ;\ P = p_o a^2 \frac{w}{3}$

$A = \frac{P}{2aw}\ ;\ Q_r = \frac{P\rho(3-2\rho)}{2aw}$

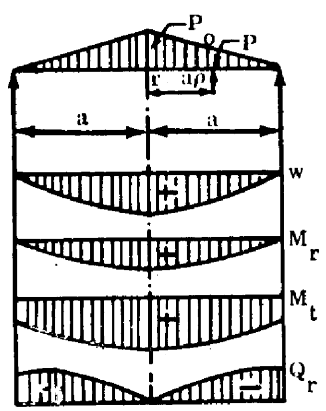

Reverse Parabolic

$p = p_o(1-\rho)^2\ ;\ P = p_o a^2 \frac{w}{3}$

$A = \frac{P}{2wa}\ ;\ Q_r = -\frac{P\rho(6-8\rho+3\rho^2)}{2aw}$

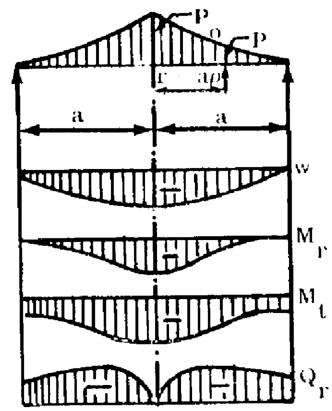

	Conical Distribution	Reverse Parabolic
w	$\frac{Pa^2}{4800D\pi}\left[\frac{3(183+43\mu)}{1+\mu} - \frac{10(71+29\mu)}{1+\mu}\right.$ $\left. -\rho^2 + 225\rho^4 - 64\rho^5\right]$	$\frac{Pa^2}{2400D\pi}\left[\frac{323+83\mu}{1+\mu} - \frac{5(89+41\mu)}{1+\mu}\rho^2\right.$ $\left. + 225\rho^4 - 128\rho^5 + 25\rho^6\right]$
β	$\frac{Pa\rho}{240D\pi}\left(\frac{71+29\mu}{1+\mu} - 45\rho^2 + 16\rho^3\right)$	$\frac{Pa\rho}{240D\pi}\left(\frac{89+41\mu}{1+\mu} - 90\rho^2 + 64\rho^3 - 15\rho^4\right)$
M_r	$\frac{P}{240D\pi}\left[71+29\mu - 45\rho^2(3+\mu)\right.$ $\left. + 16\rho^3(4+\mu)\right]$	$\frac{P}{240D\pi}\left[89 + 41\mu - 90\rho^2(3+\mu)\right.$ $\left. + 64\rho^3(4+\mu) - 15\rho^4(5+\mu)\right]$
M_r	$\frac{P}{240D\pi}\left[71+29\mu - 45\rho^2(1+3\mu)\right.$ $\left. + 16\rho^3(1+4\mu)\right]$	$\frac{P}{240D\pi}\left[89 + 41\mu - 90\rho^2(1+3\mu) +\right.$ $\left. + 64\rho^3(1+4\mu) - 15\rho^4(1+5\mu)\right]$

TABLE B7.3.3-16 SIMPLY SUPPORTED CIRCULAR PLATES (Continued)

Circumferential Loading (Linear)

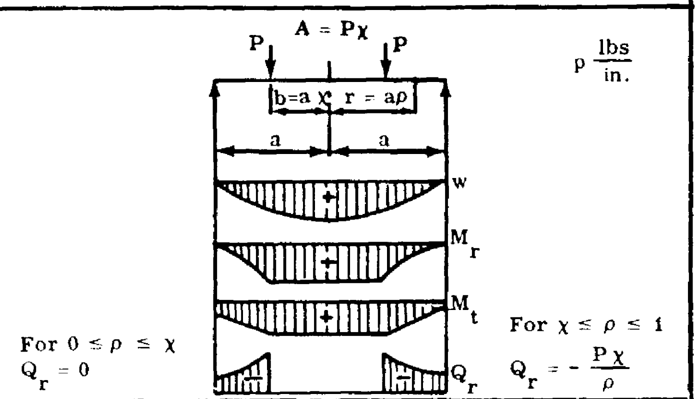

w	$\frac{Pa^3}{8D}\,\frac{\chi}{1+\mu}\left\{(3+\mu)(1+\chi^2)+(1+\mu)\chi^2\ln\chi-\left[(1-\mu)(1-\chi^2)-2(1+\mu)\ln\chi\right]\rho^2\right\}$	$\frac{Pa^3}{8D}\,\frac{\chi}{1+\mu}\left\{\left[3+\mu-(1-\mu)\chi^2\right]-(1-\rho^2)+2(1+\mu)(\chi^2+\rho^2)\ln\rho\right\}$
β	$\frac{Pa^2}{8D}\,\frac{\chi}{1+\mu}\,\rho\left[(1-\mu)(1-\chi^2)-2(1+\mu)\ln\chi\right]$	$\frac{Pa^2}{4D}\,\frac{\chi}{1+\mu}\,\rho\left[2-(1-\mu)\chi^2-(1+\mu)\frac{\chi^2}{\rho^2}-2(1+\mu)\ln\rho\right]$
M_r	$\frac{Pa\chi}{4}\left[(1-\mu)(1-\chi^2)-2(1+\mu)\ln\chi\right]$	$\frac{Pa\chi}{4}\left[(1-\mu)\chi^2\left(\frac{1}{\rho^2}-1\right)-2(1+\mu)\ln\rho\right]$
M_t	$\frac{Pa\chi}{4}\left[(1-\mu)(1-\chi^2)-2(1+\mu)\ln\chi\right]$	$\frac{Pa\chi}{4}\left\{(1-\mu)\left[2-\chi^2\left(\frac{1}{\rho^2}+1\right)\right]-2(1+\mu)\ln\rho\right\}$
Q_r	0	$-P\chi\,\frac{1}{\rho}$

TABLE B7.3.3-16 SIMPLY SUPPORTED CIRCULAR PLATES (Continued)

Circumferential Loading (Moment)

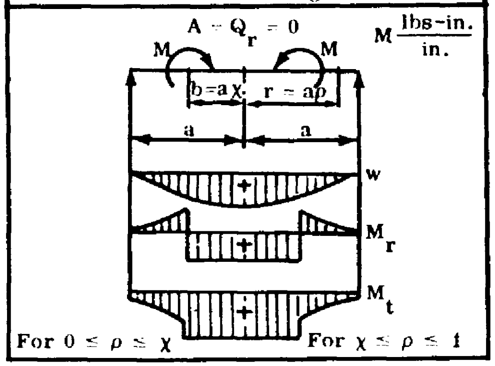

w	$\frac{Ma^2}{4D}\frac{1}{1+\mu}\left\{2\chi^2\left[1-(1+\mu)\ln\chi\right]-\left[1+\mu+(1-\mu)\chi^2\right]\rho^2\right\}$	$\frac{Ma^2}{4D}\frac{\chi^2}{1+\mu}\left[(1-\mu)(1-\rho^2)-2(1+\mu)\ln\rho\right]$
β	$\frac{Ma\rho}{2D(1+\mu)}\left[1+\mu+(1-\mu)\chi^2\right]$	$\frac{Ma\chi^2}{2D(1+\mu)}\left[(1-\mu)\rho+\frac{1+\mu}{\rho}\right]$
M_r	$\frac{M}{2}\left[1+\mu+(1-\mu)\chi^2\right]$	$\frac{M}{2}(1-\mu)\chi^2\left(1-\frac{1}{\rho^2}\right)$
M_t	$\frac{M}{2}\left[1+\mu+(1-\mu)\chi^2\right]$	$\frac{M}{2}(1-\mu)\chi^2\left(1+\frac{1}{\rho^2}\right)$
Q_r	0	0

TABLE B7. 3. 3-16 SIMPLY SUPPORTED CIRCULAR PLATES (Continued)

Partially Equal Loading

$p = \text{Const.}\ ;\ P = pb^2 w = pa^2\ w\chi^2\ ;\ A = \dfrac{P}{2aw}$

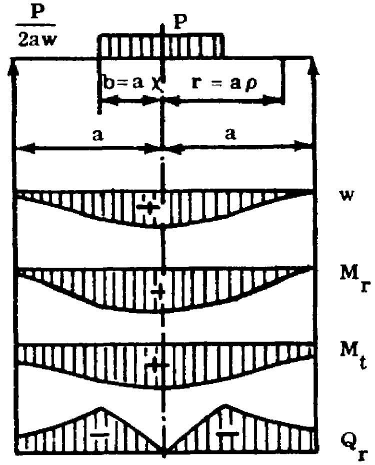

For $0 \le \rho \le \chi$

$$Q_r = -\frac{P\rho}{2a\chi^2 w}$$

For $\chi \le \rho \le 1$

$$Q_r = -\frac{P}{2aw\rho}\ .$$

w	$\frac{Pa^2}{64D\pi}\ \frac{1}{1-\mu}\left\{4(3-\mu) - (7+3\mu)\chi^2 + 4(1+\mu)\chi^2 \cdot \ln\chi\right.$ $\left. - 2\left[4-(1-\mu)\chi^2\right] - 4(1+\mu)\ln\chi \cdot \rho^2 + (1+\mu)\frac{\rho^4}{\chi^2}\right\}$	$\frac{Pa^2}{32D\pi}\ \frac{1}{1+\mu}\left\{\left[2(3+\mu) - (1-\mu)\chi^2\right](1-\rho^2) + 2(1+\mu)\chi^2\ \ln\rho + 4(1+\mu)\rho^2\ \ln\rho\right\}$
β	$\frac{Pa}{16\pi D}\ \frac{1}{1+\mu}\ \rho\left[4-(1-\mu)\chi^2 - 4(1-\mu)\ln\chi - \frac{1+\mu}{\chi^2}\ \rho^2\right]$	$\frac{Pa}{16D\pi}\ \frac{1}{1+\mu}\left\{\left[4-(1-\mu)\chi^2\right]\rho - (1+\mu)\frac{\chi^2}{\rho} - 4(1+\mu)\rho\ln\rho\right\}$
M_r	$\frac{P}{16\pi}\left[4-(1-\mu)\chi^2 - 4(1+\mu)\ln\chi - 3+\mu\right]$	$\frac{P}{16\pi}\left[(1-\mu)\chi^2\left(\frac{1}{\rho^2} - 1\right) - 4(1+\mu)\ln\rho\right]$
M_t	$\frac{P}{16\pi}\left[4-(1+\mu)\chi^2 - 4(1+\mu)\ln\chi - \frac{1+3\mu}{\chi^2}\ \rho^2\right]$	$\frac{P}{16\pi}\left\{(1-\mu)\left[4-\chi^2\left(\frac{1}{\rho^2}+1\right)\right] - 4(1+\mu)\ln\rho\right\}$

TABLE B7.3.3-16 SIMPLY SUPPORTED CIRCULAR PLATES (Concluded)

Concentrated Loading

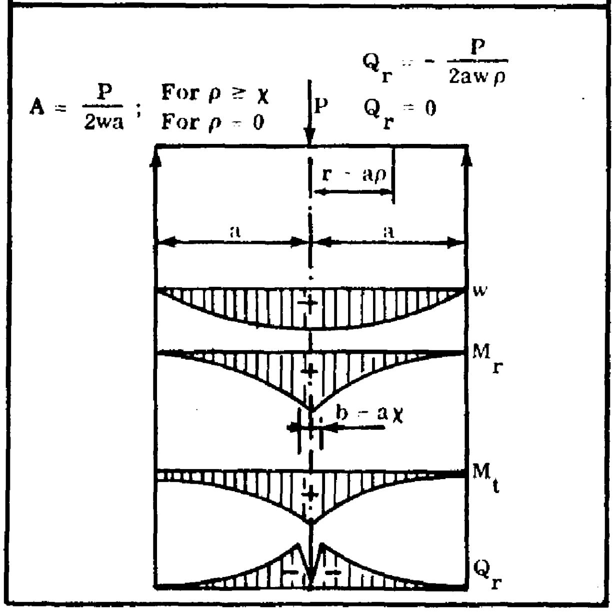

w	$\frac{Pa^2}{16D\pi}\left[\frac{3+\mu}{1+\mu}(1-\rho^2)+2\rho^2 \ln\rho\right]$
β	$\frac{Pa}{4D\pi}\rho\left(\frac{1}{1+\rho}-\ln\rho\right)$
M_r	For $\rho \geq \chi$, $-\frac{P}{4\pi}(1+\mu)\ln\rho$ For $\rho = 0$, $\frac{P}{4\pi}\left[1-(1+\mu)\ln\chi\right]$
M_t	For $\rho \geq \chi$, $\frac{P}{4\pi}\left[1-\mu-(1+\mu)\ln\rho\right]$ For $\rho = 0$, $\frac{P}{4\pi}\left[1-(1+\mu)\ln\chi\right]$

TABLE B7.3.3-17 SIMPLY SUPPORTED CIRCULAR PLATES WITH CENTRAL HOLE

Equally Distributed Loading (lb/in.²)

$$Q_r = \frac{-pa}{2}\left(\rho - \chi^2 \frac{1}{\rho}\right) ; \; A = \frac{pa}{2}(1-\chi^2); \; \chi < 1 ;$$

$$A = \frac{pa}{2}(\chi^2 - 1); \; \chi > 1 ; k_2 = \chi^2\left[3 + \mu + 4(1+\mu) \frac{\chi^2}{1+\chi^2} \ln\chi\right]$$

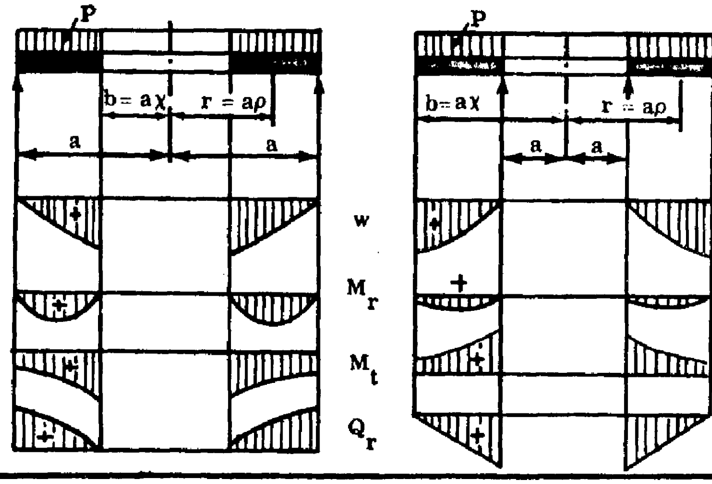

w	$\frac{pa^4}{64D}\left\{\frac{2}{1+\mu}\left[(3+\mu)(1-2\chi^2) + k_2\right](1-\rho^2) - (1-\rho^4) - \frac{4k_2 \ln\rho}{1-\mu} - 8\chi^2 \rho^2 \ln\rho\right\}$
β	$\frac{pa^3}{16D}\left[\frac{1}{1+\mu}(3+\mu - 4\chi^2 + k_2)\rho - \rho^3 + \frac{k_2}{1-\mu}\frac{1}{\rho} + 4\chi^2 \rho \ln\rho\right]$
M_r	$\frac{pa^2}{16}\left[(3+\mu)(1-\rho^2) + k_2\left(1 - \frac{1}{\rho^2}\right) + 4(1+\mu)\chi^2 \ln\rho\right]$
M_t	$\frac{pa^2}{16}\left[2(1-\mu)(1-2\chi^2) + (1+3\mu)(1-\rho^2) + k_2\left(1 + \frac{1}{\rho^2}\right) + 4(1+\mu)\chi^2 \ln\rho\right]$

TABLE B7. 3. 3-17 SIMPLY SUPPORTED CIRCULAR PLATES WITH CENTRAL HOLE (Concluded)

Concentrated Edge Loading (lb/in.)

$Q_r = P\chi/\rho$; $A = P\chi$ for $\chi < 1$; $A = -P\chi$ for $\chi > 1$

$$k_4 = 1 + \mu \frac{\chi^2}{1 + \chi^2} \ln\chi$$

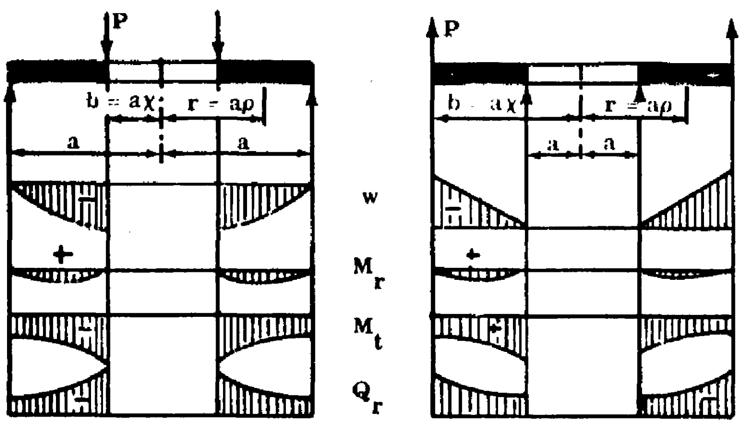

w	$\frac{Pa^3\chi}{8D}\left[\frac{3 + \mu - 2k_4}{1 + \mu}(1 - \rho^2) + 4\frac{k_4}{1 - \mu}\ln\rho + 2\rho^2 \ln\rho\right]$
β	$\frac{Pa^2\chi}{8D}\left[\frac{1 - k_4}{1 + \mu}\rho - \frac{k_4}{1 - \mu}\cdot\frac{1}{\rho} - \rho\ln\rho\right]$
M_r	$\frac{Pa\chi}{2}\left[k_4\left(\frac{1}{\rho^2} - 1\right) - (1 + \mu)\ln\rho\right]$
M_t	$\frac{Pa\chi}{2}\left[1 - \mu - k_4\left(\frac{1}{\rho^2} + 1\right) - (1 + \mu)\ln\rho\right]$

TABLE B7. 3. 3-18 SIMPLY SUPPORTED CIRCULAR PLATES WITH CENTRAL HOLE

Equally Distributed Edge Moment ($\rho = \chi$)

M is in lb-in./in.; $Q_r = 0$; $A = 0$; $k_6 = \chi^2/(1 - \chi^2)$

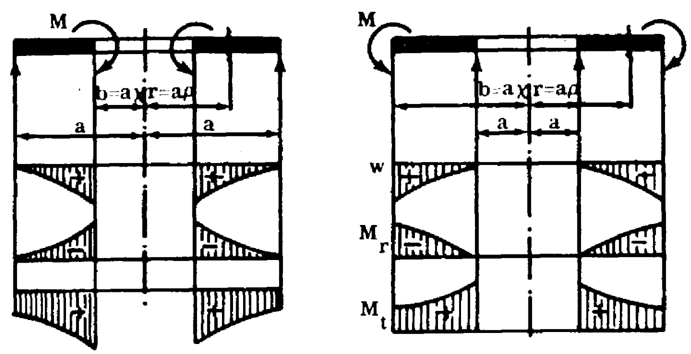

Equally Distributed Edge Moment ($\rho = 1$)

M is in lb-in./in.; $Q_r = 0 = A$; $k_7 = 1/(1 - \chi^2)$

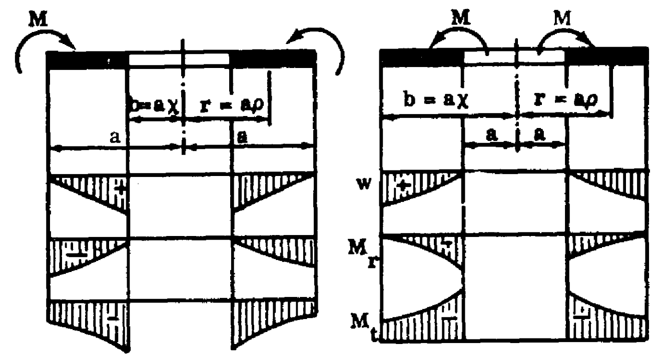

w	$\frac{Ma^2}{2D} \frac{k_6}{1+\mu} \left(1 - \rho^2 - 2 \frac{1+\mu}{1-\mu} \ln \rho\right)$	$\frac{Ma^2}{2D} \frac{k_7}{1+\mu} \left(1 - \rho^2 - 2 \frac{1+\mu}{1-\mu} \chi^2 \cdot \ln \rho\right)$
β	$\frac{Ma}{D} \frac{k_6}{1+\mu} \left(\rho + \frac{1+\mu}{1-\mu} \cdot \frac{1}{\rho}\right)$	$\frac{Ma}{D} \frac{k_7}{1+\mu} \left(\rho + \frac{1+\mu}{1-\mu} \chi^2 \cdot \frac{1}{\rho}\right)$
M_r	$Mk_6 \left(1 - \frac{1}{\rho^2}\right)$	$M\chi^2 k_7 \left(\frac{1}{\chi^2} - \frac{1}{\rho^2}\right)$
M_t	$Mk_6 \left(1 + \frac{1}{\rho^2}\right)$	$M\chi^2 k_7 \left(\frac{1}{\chi^2} + \frac{1}{\rho^2}\right)$

TABLE B7.3.3-19 CIRCULAR PLATES, STRESSES IN PLATES RESULTING FROM EDGE ELONGATION

Elongation \ Stress		
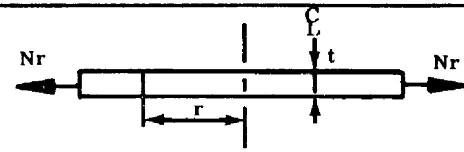		
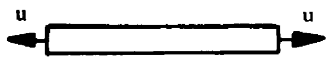	$\frac{uEt}{a(1-\mu)}$	
Elongation \ Stress	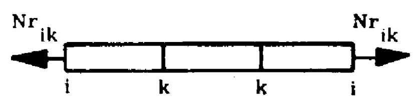	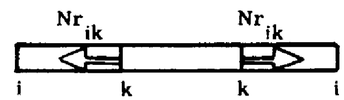
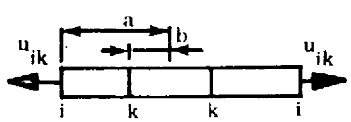	$u_{ik}\ \frac{Et(1-\lambda^{-2})}{a[1-\mu+\lambda^{-2}(1+\mu)]}$	$u_{ik}\ \frac{Et(\lambda^{2}-1)}{2a}$
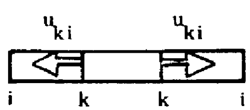	$u_{ki}\ \frac{Et(1-\lambda^{-2})}{2b}$	$u_{ki}\ \frac{Et(\lambda^{2}-1)}{b[1-\mu+\lambda^{2}(1+\mu)]}$

Note: $\lambda = \frac{a}{b}$

TABLE B7. 3. 3-20 CIRCULAR PLATE WITH CENTRAL HOLE

Equally Distributed Loading over the Surface Area

$$k_1 = \chi^2 \cdot \frac{[illegible] - \mu)\chi^2 + (1+\mu)\ (1+4\chi^2 \ln \chi)}{1-\mu + (1+\mu)\chi^2}$$

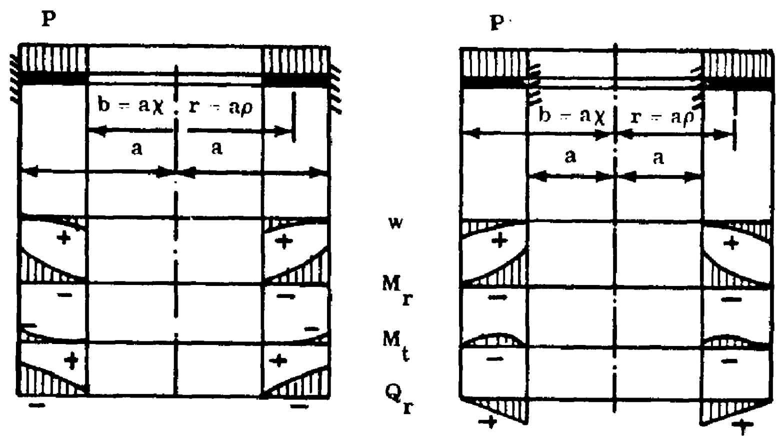

w	$\frac{pa^4}{64D}\left[-1 + 2(1 - k_1 - 2\chi^2)\ (1-\rho^2) + \rho^4 - 4k_1 \ln\rho - 8\chi^2 \rho^2 \ln\rho\right]$
β	$\frac{pa^3}{16D}\left[(1-k_1)\rho - \rho^3 + k_1 \cdot \frac{1}{\rho} + 4\chi^2 \rho \ln\rho\right]$
M_r	$\frac{pa^2}{16}\left[(1+\mu)\ (1-k_1) + 4\chi^2 - (3+\mu)\rho^2 - (1-\mu)k_1 \cdot \frac{1}{\rho^2} + 4\chi^2\ (1+\mu) \ln\rho\right]$
M_t	$\frac{pa^2}{16}\left[(1+\mu)\ (1-k_1) + 4\mu\chi^2 - (1+3\mu)\rho^2 + (1-\mu)\frac{k_1}{\rho^2} + 4(1+\mu)\chi^2 \ln\rho\right]$
Q_r	$-\frac{pa}{2}\left(\rho - \chi^2 \frac{1}{\rho}\right)$

TABLE B7.3.3-20 CIRCULAR PLATE WITH CENTRAL HOLE (Continued)

Equally Distributed Loading over the Edge Circumference

$$k_3 = \chi^2 \frac{1 + (1+\mu)\ln\chi}{1-\mu + (1+\mu)\chi^2} \qquad P\ \frac{\text{lbs}}{\text{in.}}$$

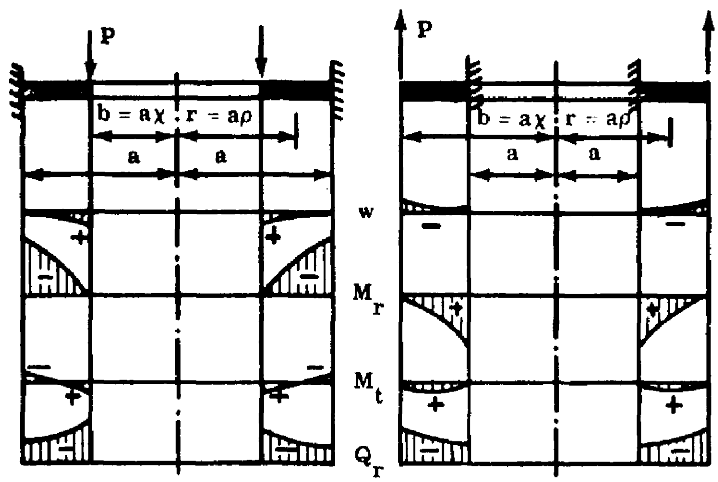

w	$\frac{Pa^3\chi}{8D}\left[(1-2k_3)(1-\rho^2) + 4k_3 \ln\rho + 2\rho^2 \ln\rho\right]$
β	$\frac{Pa^2\chi}{2D}\left[k_3\left(\rho - \frac{1}{\rho}\right) - \rho\ln\rho\right]$
M_r	$\frac{Pa\chi}{2}\left[-1 + (1+\mu)k_3 + (1-\mu)k_3\frac{1}{\rho^2} - (1+\mu)\ln\rho\right]$
M_t	$\frac{Pa\chi}{2}\left[-\mu + (1+\mu)k_3 - (1-\mu)\frac{k_3}{\rho^2} - (1+\mu)\ln\rho\right]$
Q_r	$-P\chi\frac{1}{\rho}$

TABLE B7. 3. 3-20 CIRCULAR PLATE WITH CENTRAL HOLE (Concluded)

Equally Distributed Edge Moment

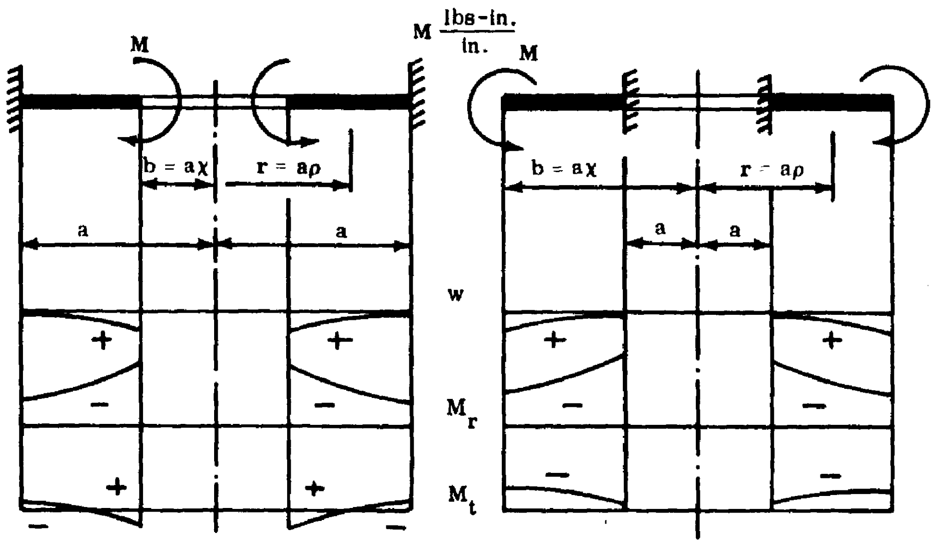

$$k_5 = \frac{\chi^2}{1 - \mu + (1 + \mu)\chi^2}$$

$$w = \frac{Ma^2}{2D} k_5(-1 + \rho^2 - 2 \cdot \ln \rho)$$

$$\beta = \frac{Ma}{D} \cdot k_5\left(\frac{1}{\rho} - \rho\right)$$

$$M_r = -M k_5\left[1 + \mu + (1 - \mu)\frac{1}{\rho^2}\right]$$

$$M_t = -M k_5\left[1 + \mu - (1 - \mu)\frac{1}{\rho^2}\right]$$

$$Q_r = 0$$

TABLE B7. 3. 3-21 CIRCULAR PLATES WITH CLAMPED EDGES

Loading Constant

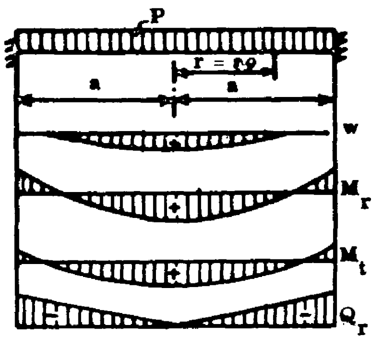

p = const. P = pa²w

Parabolic Distribution

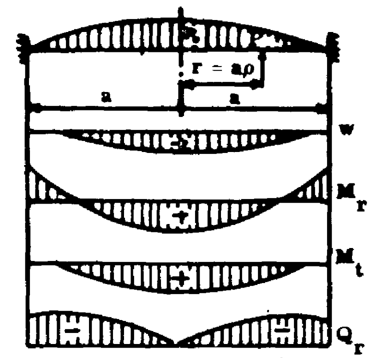

$p = P_o(1 - \rho)$ $P = \frac{1}{2} P_o a^2 w$

w	$\frac{Pa^2}{64\pi D} (1 - \rho^2)^2$	$\frac{Pa^2}{288D\pi} (7 - 15\rho^2 + 9\rho^4 - \rho^6)$
β	$\frac{Pa}{16D\pi} \cdot \rho(1 - \rho^2)$	$\frac{Pa\rho}{48D\pi} (5 - 6\rho^2 + \rho^4)$
M_r	$\frac{P}{16\pi}\left[1 + \mu - (3 + \mu)\rho^2\right]$	$\frac{P}{48\pi}\left[5(1 + \mu) - 6(3 + \mu)\rho^2 + \rho^4(5 + \mu)\right]$
M_t	$\frac{P}{16\pi}\left[1 + \mu - (1 + 3\mu)\rho^2\right]$	$\frac{P}{48\pi}\left[5(1 + \mu) - 6(1 + 3\mu)\rho^2 + (1 + 5\mu)\rho^4\right]$
Q_r	$-\frac{P}{2a\pi} \cdot \rho$	$-\frac{P}{2a\pi} \cdot \rho(2 - \rho^2)$

TABLE B7. 3. 3-21 CIRCULAR PLATES WITH CLAMPED EDGES (Continued)

Conical Distribution

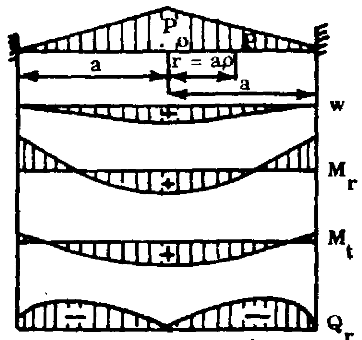

$p = P_o(1 - \rho) \qquad P = \frac{1}{3} P_o a^2 w$

Reverse Parabolic

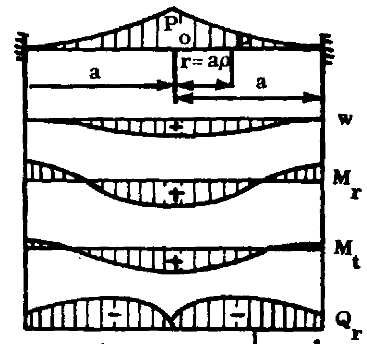

$p = P_o(1 - \rho) \qquad P = \frac{1}{6} P_o a^2 w$

	Conical Distribution	Reverse Parabolic
w	$\frac{Pa^2}{4800D\pi}(129 - 290\rho^2 + 225\rho^4 - 64\rho^5)$	$\frac{Pa^2}{4800D\pi}(83 - 205\rho^2 + 225\rho^4 - 128\rho^5 + 25\rho^6)$
β	$\frac{Pa\rho}{240D\pi}(29 - 45\rho^2 + 16\rho^3)$	$\frac{Pa\rho}{240D\pi}\left[(41 - 90\rho^2 + 64\rho^3 - 15\rho^4)\right]$
M_r	$\frac{P}{240\pi}\left[29(1+\mu) - 45(3+\mu)\rho^2 + 16(4+\mu)\rho^3\right]$	$\frac{P}{240\pi}\left[41(1+\mu) - 90(3+\mu)\rho^2 + 64(4+\mu)\rho^3 - 15(5+\mu)\rho^4\right]$
M_t	$\frac{P}{240\pi}\left[29(1+\mu) - 45(1+3\mu)\rho^2 + 16(1+4\mu)\rho^3\right]$	$\frac{P}{240\pi}\left[41(1+\mu) - 90(1+3\mu)\rho^2 + 64(1+4\mu)\rho^3 - 15(1+5\mu)\rho^4\right]$
Q_r	$-\frac{P}{2a\pi} \cdot \rho(3 - 2\rho)$	$-\frac{P}{2a\pi}\rho(6 - 8\rho + 3\rho^2)$

TABLE B7.3.3-21 CIRCULAR PLATES WITH CLAMPED EDGES (Continued)

Partially Equally Distributed Loading

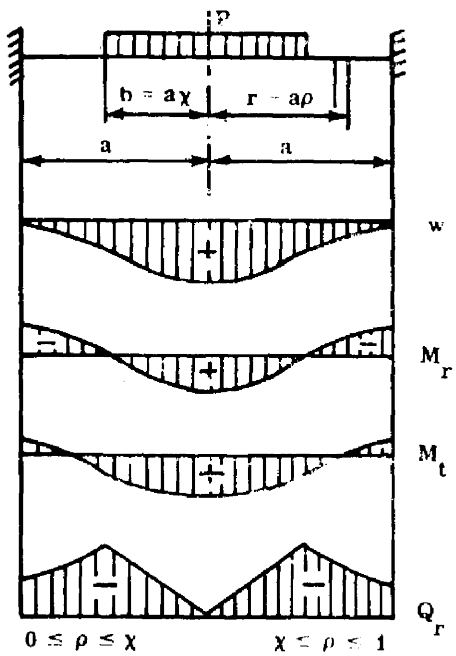

w	$\frac{Pa^2}{64D\pi}\left[4 - 3\chi^2 + 4\chi^2 \ln\chi - 2(\chi^2 - 4\ln\chi)\rho^2 + \frac{1}{\chi^2}\rho^4\right]$	$\frac{Pa^2}{32D\pi}\left[(2 - \chi^2)(1 - \rho^2) + 2(\chi^2 + 2\rho^2)\ln\rho\right]$
β	$\frac{Pa\rho}{16D\pi}\left[\chi^2 - 4\ln\chi - \frac{1}{\chi^2}\rho^2\right]$	$\frac{Pa}{16D\pi}\rho\left[\chi^2\left(1 - \frac{1}{\rho^2}\right) - 4\ln\rho\right]$
M_r	$\frac{P}{16\pi}\left[(1+\mu)(\chi^2 - 4\ln\chi) - \frac{3+\mu}{\chi^2}\rho^2\right]$	$\frac{P}{16\pi}\left[-4 + (1-\mu)\frac{\chi^2}{\rho^2} + (1+\mu)(\chi^2 - 4\ln\rho)\right]$
M_t	$\frac{P}{16\pi}\left[(1+\mu)(\chi^2 - 4\ln\chi) - \frac{1+3\mu}{\chi^2}\rho^2\right]$	$\frac{P}{16\pi}\left[-4\mu - (1-\mu)\frac{\chi^2}{\rho^2} + (1+\mu)(\chi^2 - 4\ln\rho)\right]$
Q_r	$-\frac{P}{2a\chi^2\pi}\cdot\rho$	$-\frac{P}{2a\pi}\frac{1}{\rho}$

TABLE B7. 3. 3-21 CIRCULAR PLATES WITH CLAMPED EDGES (Continued)

Concentrated Loading

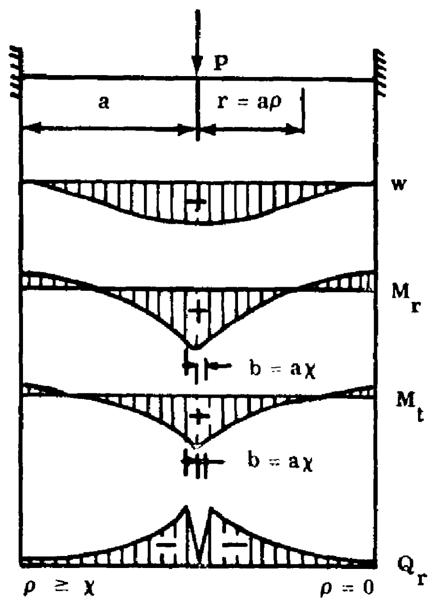

w	$\frac{Pa^2}{16D\pi}(1 - \rho^2 + 2\rho^2 \ln\rho)$	
β	$-\frac{Pa}{4D\pi}\rho\ln\rho$	
M_r	$-\frac{P}{4\pi}\left[1 + (1+\mu)\ln\rho\right]$	$-\frac{P}{4\pi}(1+\mu)\ln\chi$
M_t	$-\frac{P}{4\pi}\left[\mu + (1+\mu)\ln\rho\right]$	$-\frac{P}{4\pi}(1+\mu)\ln\chi$
Q_r	$-\frac{P}{2a\pi}\frac{1}{\rho}$	0

TABLE B7. 3. 3-21 CIRCULAR PLATES WITH CLAMPED EDGES (Continued)

Circumferential Loading (Linear)

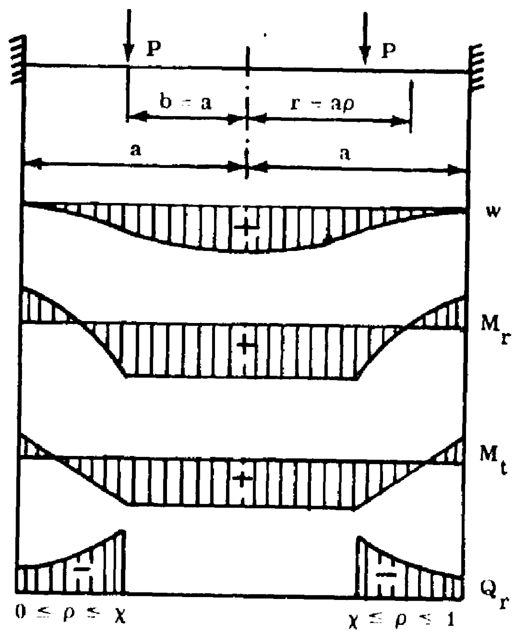

w	$\frac{Pa^3\chi}{8D}\left[1 - \chi^2 + 2\chi^2 \ln\chi + (1 - \chi^2 + 2\ln\chi)\rho^2\right]$	$\frac{Pa^3\chi}{8D}\left[(1 + \chi^2)(1 - \rho^2) + 2(\chi^2 + \rho^2)\ln\rho\right]$
β	$-\frac{Pa^2\chi\rho}{4D}(1 + \chi^{\cdot} + 2\ln\chi)$	$\frac{Pa^2\chi\rho}{4D}\left[\chi^2\left(1 - \frac{1}{\rho^2}\right) - 2\ln\rho\right]$
M_r	$-\frac{Pa}{4}\chi(1 + \mu) \cdot (1 - \chi^2 + 2\ln\chi)$	$-\frac{Pa\chi}{4}\left[2 - (1 - \mu)\frac{\chi^2}{\rho^2} - (1 + \mu)\;(\chi^2 - 2\ln\rho)\right]$
M_t	$-\frac{Pa\chi}{4}(1 + \mu) \cdot (1 - \chi^2 + 2\ln\chi)$	$-\frac{Pa\chi}{4}\left[2\mu + (1 - \mu)\frac{\chi^2}{\rho^2} - (1 + \mu)\;(\chi^2 - 2\ln\rho)\right]$
Q_r	0	$-P\chi\frac{1}{\rho}$

TABLE B7. 3. 3-21 CIRCULAR PLATES WITH CLAMPED EDGES (Concluded)

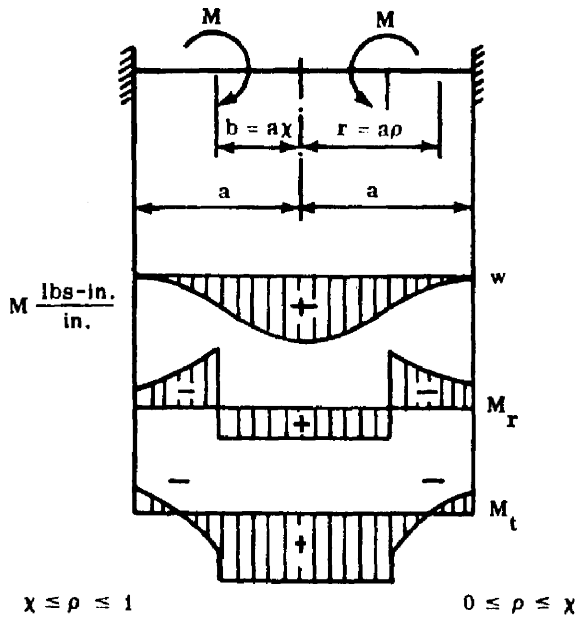

w	$-\frac{Ma^2\chi^2}{4D}(1 - \rho^2 + 2\ln\rho$	$-\frac{Ma^2}{4D}\left[2\chi^2 \ln\chi + \rho^2(1 - \chi^2)\right]$
β	$\frac{Ma\chi^2}{2D}\left(\frac{1}{\rho} - \rho\right)$	$\frac{Ma\rho}{2D}(1 - \chi^2)$
M_r	$-\frac{M\chi^2}{2}\left[1 + \mu + (1 - \mu)\frac{1}{\rho^2}\right]$	$\frac{M}{2}(1 + \mu)(1 - \chi^2)$
M_t	$-\frac{M\chi^2}{2}\left[1 + \mu - (1 - \mu)\frac{1}{\rho^2}\right]$	$\frac{M}{2}(1 + \mu)(1 - \chi^2)$
Q_r	0	0

TABLE B7.3.3-22 SYMMETRICALLY LOADED CIRCULAR RINGS

Item	Loading Condition	n > 1 Stresses	n > 1 Displacements	n = 1 Stresses	n = 1 Displacements	n = 0 Stresses	n = 0 Displacements
1	**Radial Loading** $p = p_n \cos n\theta$, where n is an integer: $n = 1, 2, 3, \ldots$ 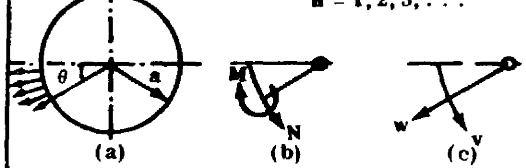 	$N = \frac{p_n a}{n^2 - 1} \cos n\theta$ $M = -\frac{p_n a^2}{n^2 - 1} \cos n\theta$	$v = -\frac{p_n a^2}{n(n^2-1)}\left(\frac{a^2}{(n^2-1) EI_2} - \frac{1}{EA}\right) \cos n\theta$ $w = \frac{p_n a^4}{(n^2-1)^2 EI_2} \cos n\theta$	Problem Does Not Exist Because the Loading Is Not in Self-Equilibrium		$N = pa$ $M = 0$	$v = 0$ $w = \frac{pa^2}{EA}$
2	**Tangential Loading** $p = p_n \sin n\theta$ 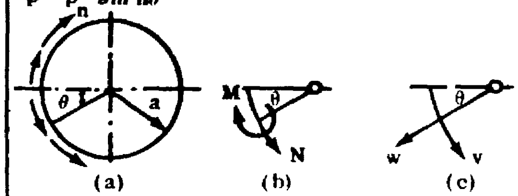 	$N = \frac{n p_n a}{n^2 - 1} \cos n\theta$ $M = \frac{p_n a}{n(n^2 - 1)} \cos n\theta$	$v = \frac{p_n a^2}{n^2 - 1}\left[\frac{a^2}{n^2(n^2-1) EI_2} + \frac{1}{EA}\right] \sin n\theta$ $w = -\frac{p_n a^4}{n(n^2-1)^2 EI_2} \cos n\theta$	Problem Does Not Exist Because the Loading Is Not in Self-Equilibrium		Problem Does Not Exist Because the Loading Is Not in Self-Equilibrium	
3	**Loading Normal to the Plane of the Ring** $p = p_n \cos n\theta$ 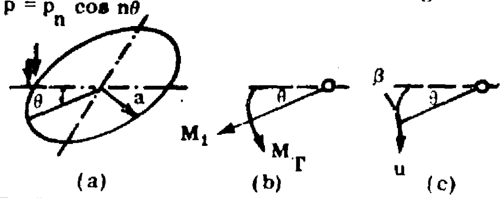 	$M_1 = \frac{p_n a^2}{n^2 - 1}$ $M_T = -\frac{p_n a^2}{n(n^2 - 1)} \sin n\theta$	$u = \frac{p_n a^4}{(n^2-1)^2}\left[\frac{1}{EI_1} + \frac{1}{n^2 GJ}\right] \cos n\theta$ $\beta = \frac{p_n a^3}{(n^2-1)^2}\left[\frac{1}{EI_1} + \frac{1}{GJ_T}\right] \cos n\theta$	Problem Does Not Exist Because the Loading Is Not in Self-Equilibrium		Problem Does Not Exist Because the Loading Is Not in Self-Equilibrium	
4	**External Moments, About the Ring Axis** $m = m_n \cos n\theta$ 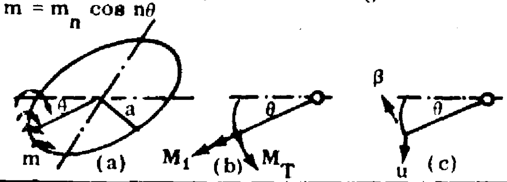 	$M_1 = \frac{m_n a}{n^2 - 1} \cos n\theta$ $M_T = \frac{n m_n a}{n^2 - 1} \cos n\theta$	$u = \frac{m_n a^3}{(n^2-1)^2}\left[\frac{1}{EI_1} + \frac{1}{GJ}\right] \cos n\theta$ $\beta = \frac{m_n a^2}{(n^2-1)^2}\left[\frac{1}{EI_1} + \frac{n^2}{GJ}\right] \cos n\theta$	Problem Does Not Exist Because the Loading Is Not in Self-Equilibrium		$M_1 = ma$ $M_T = 0$	u = May Assume Any Desired Value $\beta = \frac{ma^2}{EI_1}$

$$w = \frac{Ma^2}{2D(1+\mu)}(1-\rho^2)$$

$$\beta = \frac{Ma}{D(1+\mu)} \cdot \rho$$

$$M_r = M_t = M$$

$$Q_r = 0$$

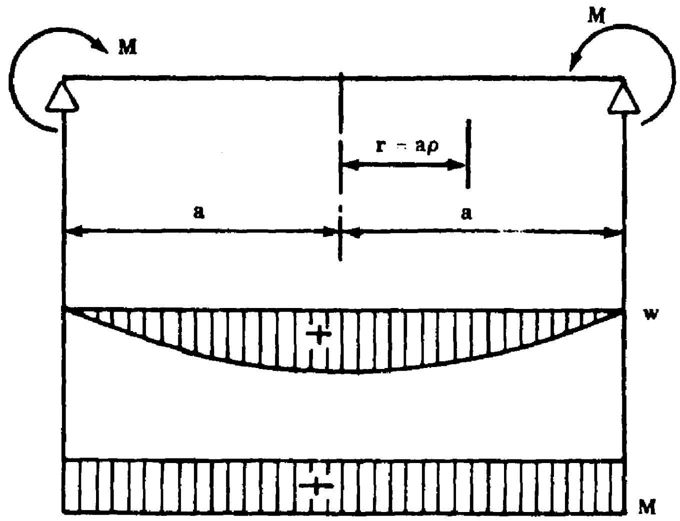

FIGURE B7.3.3-7 FORMULAS OF INFLUENCES FOR A SIMPLY SUPPORTED CIRCULAR PLATE LOADED WITH EQUALLY DISTRIBUTED END MOMENT

B7.3.3.7 Circular Rings

Circular rings are important structural elements which often interact with shells. The theory of shells would not be complete without information about circular rings. In this section, such information is summarized and presented for symmetrical loading with respect to the center of the ring.

Nomenclature employed is as follows:

A = area of the cross section

I_1, I_2 = moment of inertia for the centroidal axis in the plane or normal to the plane of the ring

J = torsional rigidity factor of the section.

Table B7.3.3-22 presents the solutions for different loads on rings.